

MASTER THESIS

Thesis submitted in partial fulfillment of the requirements
for the degree of Master of Science in Engineering at the
University of Applied Sciences Technikum Wien

Degree Program in Tissue Engineering and Regenerative
Medicine

Characterizing hepatocyte turnover in homeostasis and injury

By: Esther Dolz, BSc
Student Number: 1810692025

Supervisor 1: Dr. Kristin Knouse, MD, PhD

Supervisor 2: Heidemarie Fuchs, PhD

Boston, 12/10/2020



Declaration of Authenticity

“As author and creator of this work to hand, I confirm with my signature knowledge of the relevant copyright regulations governed by higher education acts (see Urheberrechtsgesetz/ Austrian copyright law as amended as well as the Statute on Studies Act Provisions / Examination Regulations of the UAS Technikum Wien as amended).

I hereby declare that I completed the present work independently and that any ideas, whether written by others or by myself, have been fully sourced and referenced. I am aware of any consequences I may face on the part of the degree program director if there should be evidence of missing autonomy and independence or evidence of any intent to fraudulently achieve a pass mark for this work (see Statute on Studies Act Provisions / Examination Regulations of the UAS Technikum Wien as amended).

I further declare that up to this date I have not published the work to hand nor have I presented it to another examination board in the same or similar form. I affirm that the version submitted matches the version in the upload tool.”

Boston, September 2, 2020

Place, Date

Esther Dolz Cerdá

Signature

Abstract

The mammalian liver is the largest organ in the body and is responsible for numerous functions that impact all systems in the body. Unlike any other internal organ, the liver can completely regenerate itself after injury. This regeneration is not driven by a stem cell population but by the proliferation of differentiated hepatocytes. The liver shows a high regenerative capacity, being capable of repairing up to 70% of lost tissue within a few weeks. Following moderate to severe injury, different hepatocytes re-enter the cell cycle, proliferate and restore the lost tissue. It is the hepatocytes themselves that proliferate to regenerate the liver. Although this property of the liver has been known for decades, it is still not clear how hepatocytes in homeostasis are able to regenerate the liver after severe injury. Some studies suggest that select hepatocytes distributed throughout the liver lobule have heightened proliferative capacity, others indicate that hepatocytes located in the pericentral zone are the source of all new hepatocytes and yet others suggest that all hepatocytes have equivalent proliferative capacity.

With this project, we want to try to understand the behaviors and pathways that different hepatocytes engage to regenerate the liver. For this, tissue processing, immunofluorescence and imaging were performed, and it was determined that there is not a specific location for the proliferation of hepatocytes but that they appear to proliferate at random locations. This led to the early conclusion that there is not one specific zone where proliferation takes place and follows the conclusion drawn by other studies that it is unlikely that there is one specific zone where proliferation occurs. However, it remains possible that some hepatocytes are still more proliferative than others but that they are distributed across the concentric zones of the liver.

Another experiment was performed to locate the fate of proliferative hepatocytes. For this, Ki67CreER;tdTomato mice were pulsed 2mg tamoxifen injections every other day for one month. After one month, the mice were kept alive for two more weeks with no tamoxifen injections just to let all tamoxifen wash out from the system to prevent the labelling of new proliferative hepatocytes. If it is true that there are some hepatocytes that are more likely to proliferate, then the cells that are actively proliferating at the time of harvest should be more likely to have proliferated in the month of labelling. It was shown that this double positive hepatocytes (Ki67+tdTomato+) were located no more than 4 cells away from the central vein which suggests that these double-positive hepatocytes are spatially restricted to the central vein zone as also mentioned in other studies.

Acknowledgements

First, I would like to thank both of my supervisors, Kristin Knouse and Heidemarie Fuchs for guiding me on this research project.

Thank you, Marshall Plan Scholarship, for helping me fulfill my dream of doing my internship at the Whitehead Institute for Biomedical Research.

Thank you to the Whitehead Institute for Biomedical Research and Dr. Knouse's laboratory for making this possible.

To you, mom and dad, for being the fundamental pillar in all I am, for your unconditional support throughout these years and for your love. Without you this would have not been possible. Thank you for believing in me.

To you, Belenchi and Migue, for teaching me so much. You are one of the engines that drive me to be better every day so that you will always feel proud.

To my best friend, Bea, for being the best support during these last years and especially during this global pandemic. We both know this would have been very different if we had not had each other. Thank you for putting up with me in my worst moments and for being by my side. Looking forward to collecting more memories by your side.

To you my love, for supporting me unconditionally until the very last moment. For not letting me break down in the worst moments. For teaching me what is truly important in life. This is, in big part, thanks to you.

And finally, to those who are gone, with the only intention of making you feel proud. Always in my heart.

Table of Contents

| | | |
|-----------|--|--------------------------------------|
| 1 | Introduction..... | 5 |
| 1.1 | The mammalian liver | 5 |
| 1.1.1 | Architecture of the Liver and Biliary Tract..... | 5 |
| 1.1.1.1 | Hepatic vascular system | 6 |
| 1.1.1.2 | Biliary system | 9 |
| 1.1.1.3 | Architecture of hepatic tissue | 11 |
| 1.1.2 | Hepatocytes | 12 |
| 1.1.2.1 | Morphology | 13 |
| 1.1.2.2 | Function | 14 |
| 1.1.3 | Regenerative potential..... | 15 |
| 1.1.3.1 | Natural causes of liver injury | 15 |
| 1.1.3.2 | Experimental systems to causes liver injury..... | 16 |
| 1.1.3.3 | Pathways of liver regeneration after PHx..... | 18 |
| 1.1.3.3.1 | Priming or initiation phase | 19 |
| 1.1.3.3.2 | NF-KB signaling pathway | 20 |
| | Role of innate immunity components | 20 |
| | Role of tumor necrosis factor alpha (TNFa) | 20 |
| 1.1.3.3.3 | Wnt/beta cantenin signaling pathway | 21 |
| 1.1.3.3.4 | Notch signaling pathway | 21 |
| 1.1.3.3.5 | Proliferation phase | 22 |
| 1.1.3.3.6 | Termination phase..... | 22 |
| | Transforming growth factor β (TGF- β) | 22 |
| 1.2 | Actual regenerative theories | 23 |
| 2 | Methodological considerations..... | 26 |
| 2.1 | Used antibodies | 26 |
| 2.2 | Immunofluorescence..... | jError! Marcador no definido. |
| 2.3 | Lineage tracing | 27 |
| 3 | Workflow..... | jError! Marcador no definido. |
| 3.1.1 | Characterizing the location of hepatocyte proliferation and death..... | 24 |
| 3.1.2 | Trace the fate of proliferative hepatocytes | 25 |
| 4 | Methods | 28 |
| 4.1 | Creating liver tissue samples..... | 29 |
| 4.2 | Locating proliferative hepatocytes in thick liver tissue..... | 32 |
| 4.3 | Lineage tracing of proliferative hepatocytes | 33 |
| 5 | Results | 35 |
| 5.1 | Hepatocyte proliferation does not follow a specific pattern | 35 |
| 5.2 | Fate of proliferative hepatocytes | 41 |
| 6 | Discussion..... | 44 |

| | |
|---|---|
| <i>Bibliography.....</i> | <i>47</i> |
| <i>List of Figures.....</i> | <i>53</i> |
| <i>List of Tables.....</i> | <i>55</i> |
| <i>List of Abbreviations.....</i> | <i>56</i> |
| <i>A: Protocols</i> | <i>57</i> |
| <i>A.1 Immunostaining and clearing tissue slices</i> | <i>57</i> |
| <i>A.2 Immunostaining</i> | <i>58</i> |
| <i>B: Heading of Appendix B.....</i> | <i>¡Error! Marcador no definido.</i> |

1 Introduction

Adult tissues depend on endocrine, secretory and metabolic functions to maintain function and mass. In tissues with high turnover such as skin, intestine, and blood, there are distinct compartments of stem cells that sustain regular turnover. The liver is the only internal organ able to regenerate itself- however, in quiescent tissues such as liver and pancreas, the existence of specialized stem cells and cell niches is questionable [1]. The liver shows a high regenerative capacity, being capable of repairing up to 70% of lost tissue within a few weeks. Following moderate to severe injury, different hepatocytes re-enter the cell cycle, proliferate and restore the lost tissue [2].

1.1 The mammalian liver

The mammalian liver is the largest organ in the body and is responsible for numerous functions that impact all systems in the body. These functions can be classified into three fundamental roles, (i) Vascular function, including formation of the hepatic phagocytic and lymph system; (ii) secretory and excretory, especially with reference to the synthesis of bile secretion; (iii) metabolic achievements in control of utilization and synthesis of proteins, lipids and carbohydrates [3]. A major consequence of these fundamental roles is that hepatic disease has widespread effects on all other organ systems.

1.1.1 Architecture of the Liver and Biliary Tract

Human liver does not reach mature architecture until 15 years of age. The liver is about a 2% of the total body weight of an adult. The liver lies in the abdominal cavity and its mass is divided into different lobes. The size and number of liver lobes vary among species. In most mammals the gallbladder is seen attached to the liver (Figure 1). The common bile duct (Figure 1), delivers bile from both the gallbladder and the liver into the duodenum [4].

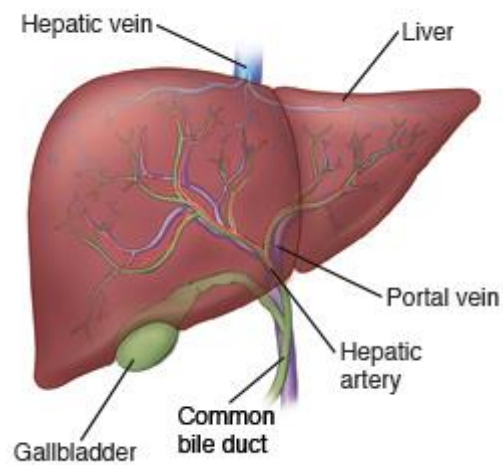


Figure 1. Anatomy of the liver [5].

The major aspects of the hepatic structure are the, (i) hepatic vascular system; (ii) biliary tree, and (iii) the three-dimensional arrangements of the liver cells.

1.1.1.1 Hepatic vascular system

The majority of the liver's blood, roughly 75%, is supplied by the portal vein. All the venous blood returning from the stomach, pancreas, spleen, and small intestine converges into this portal vein. The remaining 25% of the supplied blood is from the hepatic artery. (Figure 2). [2]

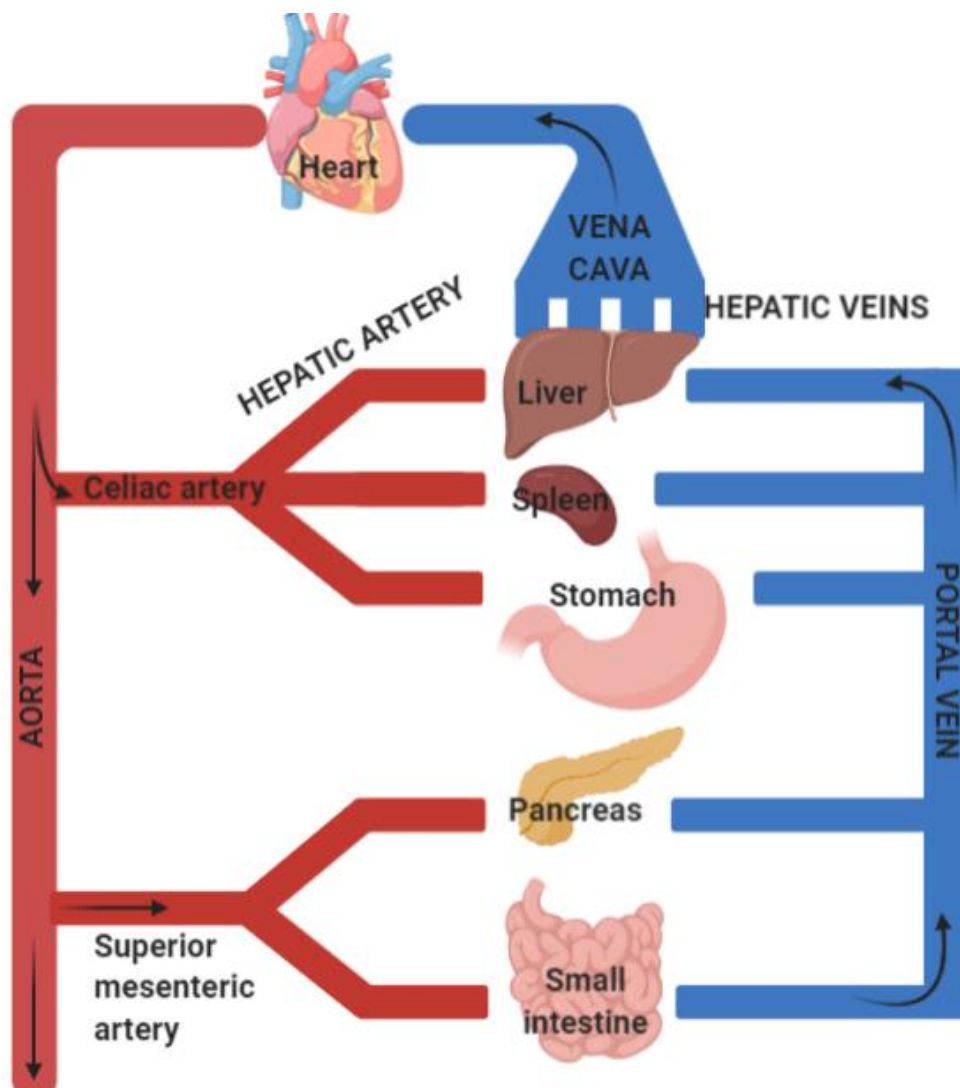


Figure 2. Blood flow showing the supplied blood to the liver from the hepatic artery and portal vein.

The liver is located strategically, downstream of the blood flow from the intestine, to receive absorbed nutrients and harmful absorbed molecules like bacterial toxins or drugs [6]. The liver extracts the toxic metabolic products that have been produced elsewhere in the body by converting them to chemical forms so they can be excreted.

Terminal branches of the hepatic artery and portal vein empty together and mix as they enter the liver sinusoids. These are distensible vascular channels coated with fenestrated endothelial cells and surrounded circumferentially by hepatocytes. As the blood flows through these sinusoids, plasma is filtered into the space of Disse, space between the hepatocytes and endothelial cells, providing a considerable fraction of the body's lymph [7]. Blood flows through the sinusoids emptying into each lobules central vein [3]. (Figure 3)

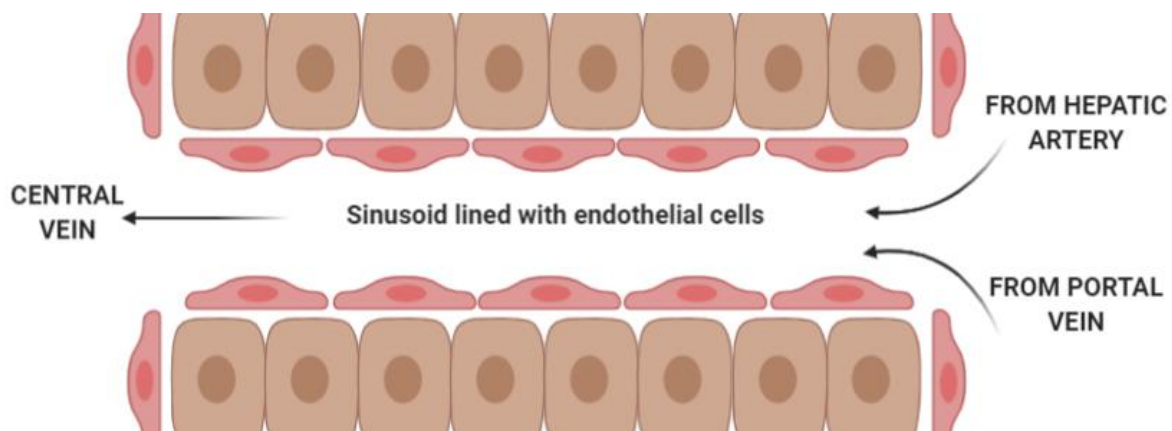


Figure 3. Architecture of the liver and biliary tract. Blood flows through the liver sinusoids emptying into the central vein of each lobule. (Image created with Biorender application).

There are different types of cells in the hepatic sinusoids. These cells are non-parenchymal cells (NPCs). The main cell found in the hepatic sinusoid is the liver sinusoidal endothelial cell (LSEC). The other cells found in the hepatic sinusoids are resident cells, cells that can be found in the liver as well as in many other sites of the body [8][9].

LSECs have gaps between them. They do not have a basement membrane and they have many fenestrations on their surface [10]. This structure allows rapid exchange of macromolecules from plasma in passage to hepatocytes [11]. Red blood cells remain in the sinusoids but other plasma cells as big as albumin pass through this barrier [12].

Kupffer cells (KCs) are the main residence cells of the sinusoids. They can be found in the cell membrane of the LSECs, but bulge into the sinusoid's lumen [13]. There are also macrophages which are responsible for phagocytosis and of the secretion of a number of substances such as cytokines [10].

The space between the hepatocytes and the LSECs is the space of Disse or perisinusoidal space (Figure 4). This space is composed by many proteins found in the extracellular matrix of different tissues of the body. The perisinusoidal space provides physical support to the hepatocyte plates as they do not have a basement membrane [14]. Stellate cells are the main NPCs in the space of Disse and its main function is vitamin A storage [11] [15]. In a healthy liver, stellate cells are quiescent. When the liver becomes injured by a virus infection or by toxins, immune cells and hepatocytes release factors that force stellate cells to undergo a transformation known as the activated state. When they are activated, they start to secrete extracellular matrix proteins like glycoproteins, proteoglycans, and collagens. This process of activation is associated with loss of vitamin A storage. This response protects and facilitates healing of a damaged liver. However, when the source of injury is chronic, stellate cells

stay activated and secrete collagen to a point in which the liver becomes fibrotic and thus hepatic function declines. [16][17][18]

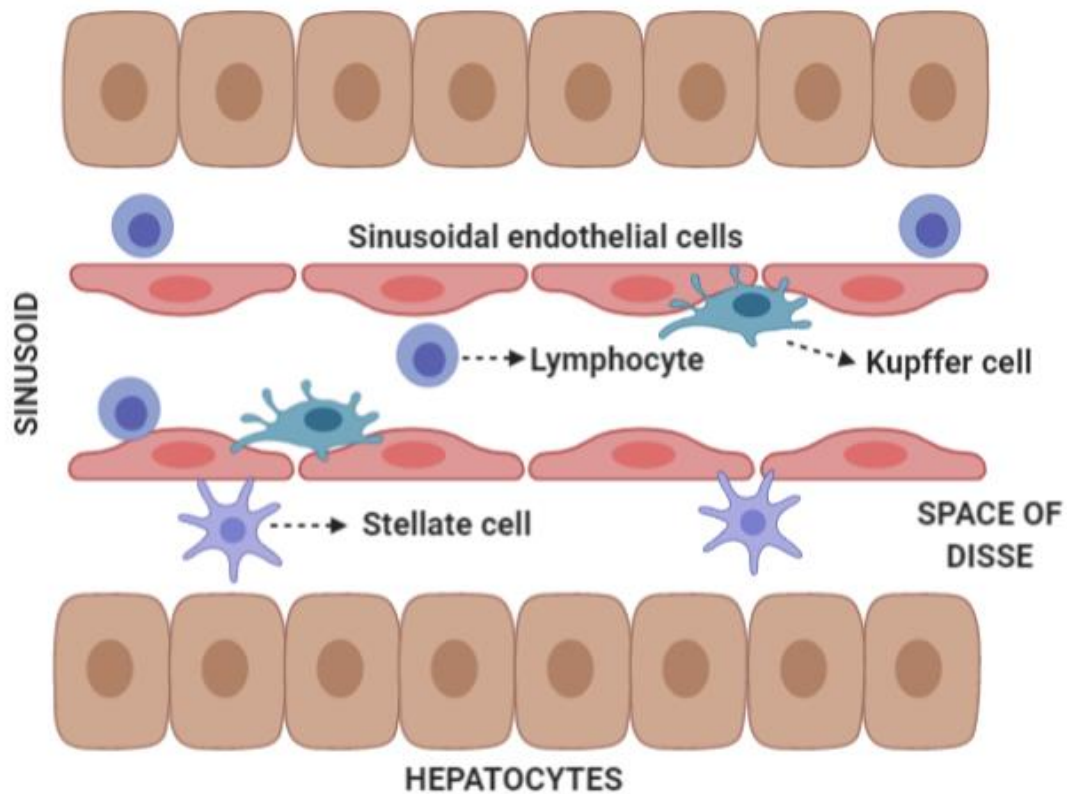


Figure 4. Structure of the liver. Hepatic sinusoids are formed by Kupffer cells and sinusoidal endothelial cells. Hepatocytes are localized in the space of Disse, outside of the sinusoid. (Image created using Biorender application).

1.1.1.2 Biliary system

The biliary system is a series of ducts and channels that carry bile, an excretory and secretory product of hepatocytes, from the liver to the small intestine lumen. Hepatocytes are arranged in plates with their apical surfaces surrounding and facing the sinusoids. The basal faces of contiguous hepatocytes are linked together by junctional complexes to form the canaliculi, the first canal of the biliary system. A bile canaliculus is not a duct, but the intercellular space enclosed by adjacent hepatocytes [19] [20].

Hepatocytes secrete bile in the canaliculi, and these secretions flow in parallel to the sinusoids, but opposite to blood flow direction. At the ends of the canaliculi, bile flows into the bile ducts, coated with epithelial cells. Therefore, the bile ducts begin very close to the terminal branches of the hepatic artery and portal vein, and this group of structures is an important

and easily recognizable landmark seen in liver histological sections: the bile duct group (Figure 5). The portal triad is the grouping of the portal venule, bile duct and hepatic arteriole [14] [15] [21].

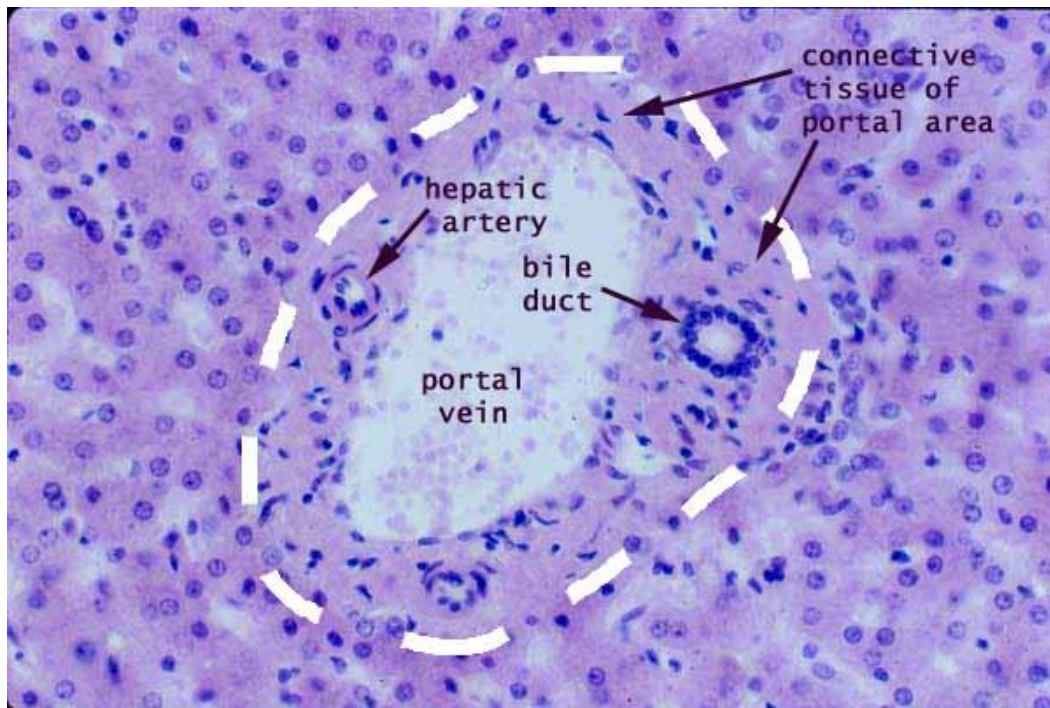


Figure 5. Histological view of the portal triad. Hepatic artery, Bile duct and portal vein [21].

Both bile ductules and bile ducts have specialized epithelial cells known as cholangiocytes. They modify and process the bile as it flows through the ducts [15].

1.1.1.3 Architecture of hepatic tissue

The liver is composed of smaller structures known as lobules. Each of the lobules is surrounded by branches of the portal vein and the hepatic artery. These vessels drain into the sinusoids, to exchange materials with the hepatocytes. The sinusoids drain into the central vein which responsible to feed deoxygenated blood to the hepatic vein. Hepatocytes produce bile, transported then by the canaliculi to the bile ducts located surrounding the lobule. [22]

The lobule is the hepatic structural unit. It consists of a hexagonal arrangement of hepatocyte plates radiating from a central vein. At each of the vertices of the lobule there are portal triads distributed regularly. These portal triads contain a portal vein, an hepatic artery terminal branch and a bile duct [2] [22]. (Figure 6).

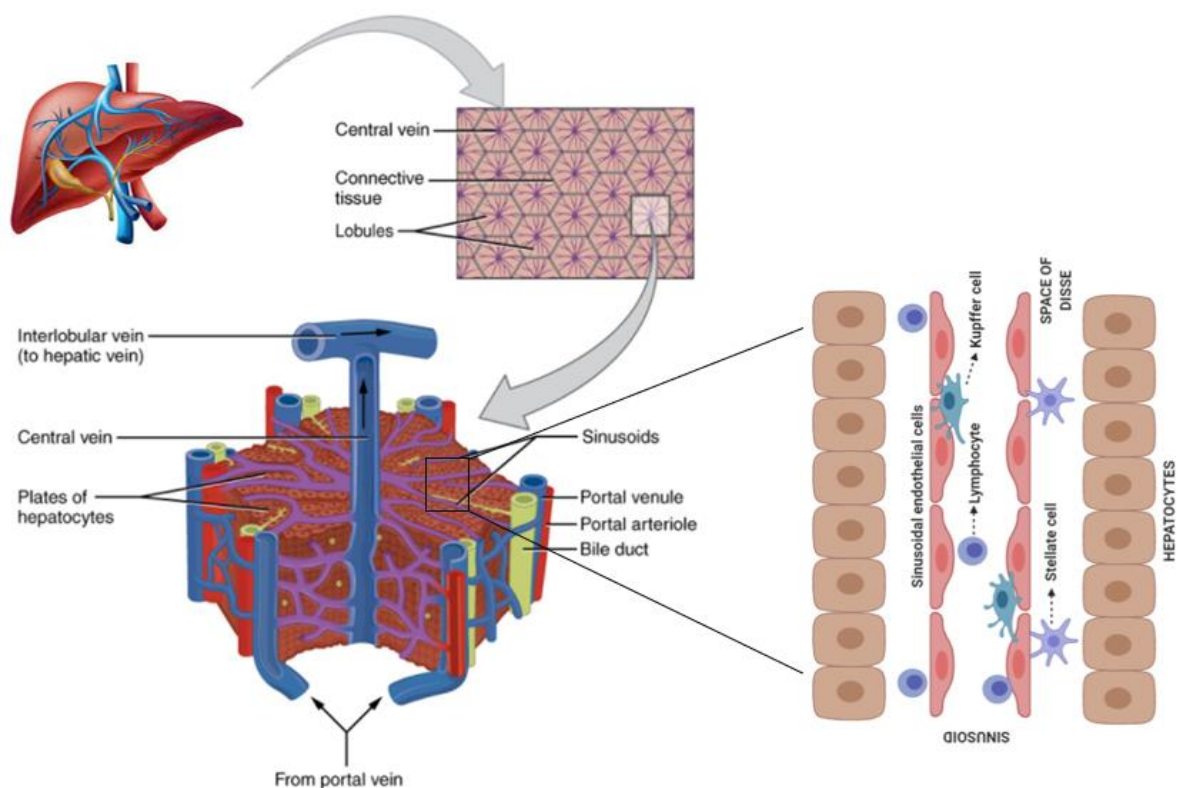


Figure 6. Structure of the functional units, lobules, of the liver. Adapted from [23].

1.1.2 Hepatocytes

Hepatocytes are the liver parenchymal cells. They are the cells responsible for most of the liver functions. Hepatocytes constitute between 60% and 80% of the mass of the liver [24] [25]. They are arranged in sheets of one cell in thickness. These sheets connect to each other forming a spongy-like structure (Figure 7). Hepatocytes renew every five months, however under regenerative processes this may change, hepatocytes will then show a high ability for regeneration and proliferation [26].

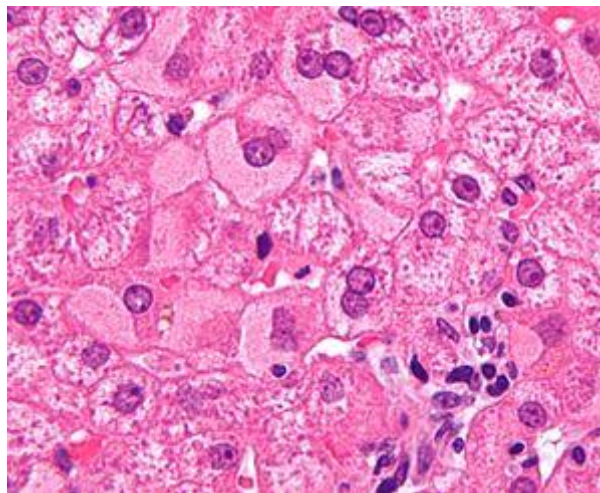


Figure 7. Arrangement of hepatocytes in sheets of one cell in thickness. [27]

From a metabolic perspective, hepatocytes located in the periportal zone (zone 1) are specialized in β -oxidation and gluconeogenesis, while hepatocytes that are in zone 3, around the central vein are more important for detoxification, lipogenesis, and glycolysis. Therefore, hepatocytes are heterogeneous regarding their functions. Depending on their location across the hepatic lobule, they express different genes. This metabolic zonation allows the liver to respond to different hepatotoxins or nutritional requirements—[28]. Halpern et al. obtained in 2018 the zonation profiles with high spatial resolution of all liver genes. They found out that around 50% of the liver genes uncover abundant non-monotonic profiles peaking at the mid-lobule layers, and are significantly zoned [29].

1.1.2.1 Morphology

Hepatocytes are polyhedral cells, usually showing 6 faces. These faces are always in contact with either a sinusoid or another hepatocyte [26]. These cells may either be mono or binucleated (Figure 8). The majority of hepatocyte nuclei are tetraploid, containing double the amount the DNA than a normal cell. The nuclei are usually round and big. The characteristics of the cytoplasm vary depending on the cells physiological state which will be influenced by glycogen and fat depots. Hepatocytes contain many small mitochondria, about 50 Golgi apparatuses organized in stacks of 3-5 cisterns, many peroxisomes and many lysosomes near the biliary canaliculi (Figure 8). [30]

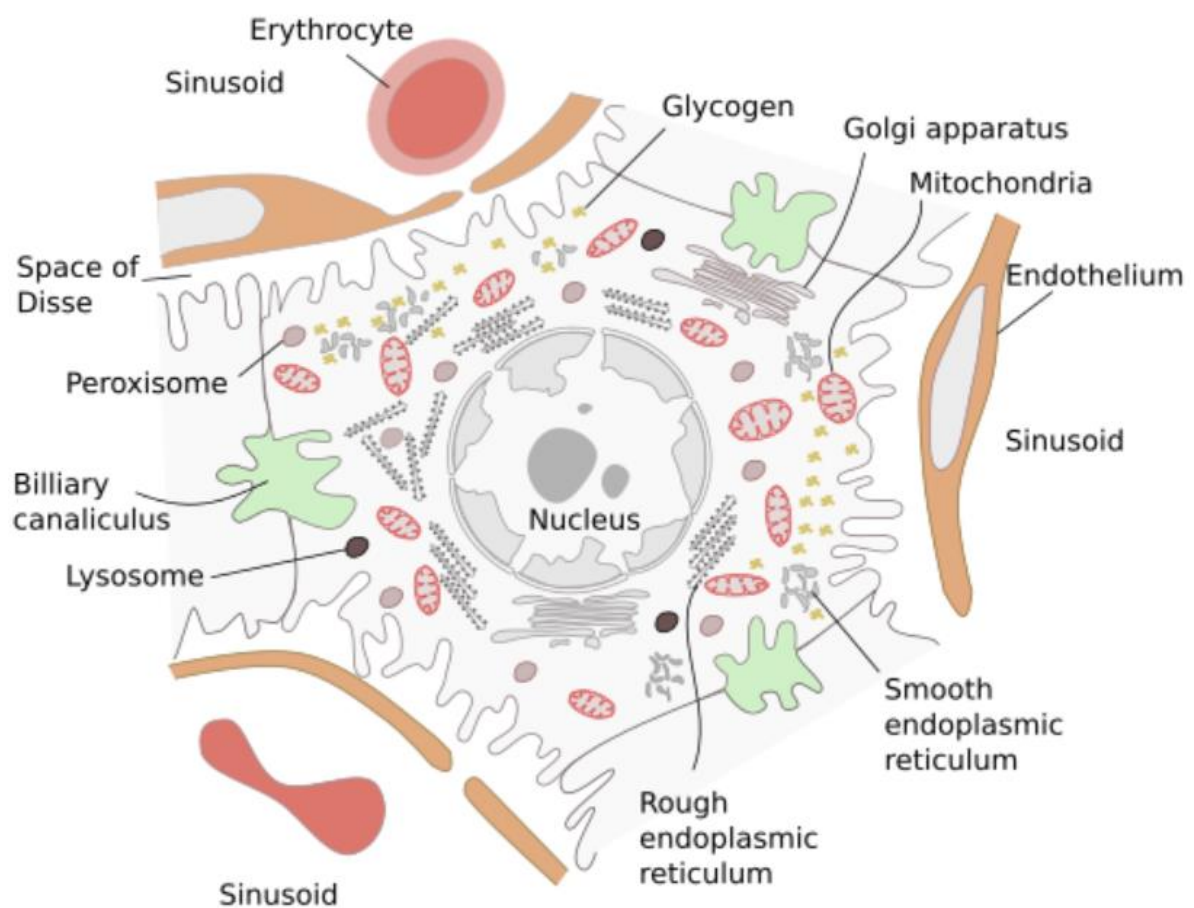


Figure 8. Ultrastructure of hepatocyte cells. [23]

Abundant lipid and glycogen depots are found in the cytoplasm of hepatocytes. Residual bodies containing lipofuscin can also be found in the cytoplasm of these cells [31].

Hepatocytes have lateral, apical and basal domains, like epithelial cells in general, which determine cell alignment in the lobule plates, as well as the bile flow [32].

Each cell has 2 matching basal surfaces at opposite ends of the cell. These domains face the sinusoids allowing substances to enter the cell from the blood [33] [34].

The lateral or side face of each joins to the cell directly adjacent to that domain. Halfway between the two basal domains there is a surface that allows the bile produced by a cell to exit the cell. This surface is known as the apical domain [35].

1.1.2.2 Function

The main function of hepatocytes is to metabolize substances absorbed from the digestive tract. These cells are also involved in the detoxification of harmful molecules. Additionally, hepatocytes synthesize bile which is released in the intestine and helps with digestion. For both of these functions, hepatocytes are placed in contact with sinusoids, which form the bile canaliculi to drain the bile from the liver lobules [36].

Hepatocytes take up the glucose molecules originally absorbed by the digestive tract and store them as glycogen which is mobilized when the body needs energy [26].

Bile salts are one of the substances that are synthesized by hepatocytes. In the smooth endoplasmic reticulum (SER), many enzymes are involved in cholesterol and other lipids synthesis. Additionally, hepatocytes produce lipoproteins which are needed for lipid transport in the blood stream. Plasma albumins and fibrinogen, for blood clotting, are also synthesized in hepatocytes. Hepatocytes store heparin and vitamins A and B [37].

Hepatocytes are also the first to receive toxic and harmful substances. Ethanol of alcoholic drinks is degraded in the peroxisomes found in the hepatocytes. There are enzymes in the SER involved in the inactivation or degradation of drugs and toxins. During periods of continuous alcohol drinking or medicine treatments, the endoplasmic reticulum becomes the bulkiest organelle of hepatocytes [31].

The liver is the second major center for production of heme groups pro after the bone marrow. Heme group is a non peptidic group found in different proteins for oxygen transportation, in enzymes like peroxidases and catalases that protect against oxidative substances. Additionally, it is part of the peroxisomal and mitochondrial cytochromes [23] [38].

Hepatocytes regulate the systemic body concentration of iron by releasing the hepcidin hormone. Hepcidin controls the plasma iron by favoring the degradation and internalization of ferroportin, an iron transporter found in macrophages, hepatocytes and enterocytes. Ferroportin removal inhibits the iron release from these cells. This hormone synthesis is regulated

by the concentration of transferrin-iron in the plasma, by inflammation and by iron deposits in hepatocytes [38] [39].

1.1.3 Regenerative potential

The liver has a remarkable capacity to regenerate after damage or injury. In skin and intestines, epithelial tissues with a high turnover, tissue homeostasis and cellular renewal is carried out by a pool of stem cells. Liver has slow turnover and there is not believed to be a stem cell population, rather all hepatocytes are derived from pre-existing hepatocytes [40]. Hepatocytes are clearly not terminally differentiated cells as they appear to have unlimited proliferative capacity [11].

1.1.3.1 *Natural causes of liver injury*

The liver is the main site for alcohol metabolism and therefore susceptible to injury following excessive alcohol consumption. Liver's susceptibility to alcohol-induced toxicity is due to both the metabolic consequences of ethanol metabolism, as well as the high concentration of alcohol in the portal blood. Alcoholic Liver Disease (ALD) is a spectrum of different diseases that include fatty liver (steatosis), fibrosis, cirrhosis, and steatohepatitis. Steatosis is characterized by the accumulation of fat in hepatocytes and develops in 90% of individuals who drink large doses of alcohol, however, it can resolve upon cessation of alcohol intake [41][42]. Only in a minority of individuals who drink heavily, steatosis can progress to steatohepatitis, which is a combination of persistent steatosis accompanied by inflammation. Alcohol consumption alone does not cause ALD progression from steatosis to steatohepatitis, fibrosis or, cirrhosis; rather, a second insult or risk factor is required for the development of the later stages of disease. Such second risk factors could include hypoxia, reactive oxygen species or inflammatory responses, among others. Acute ethanol exposure, for example, is known to enhance liver pathology induced by bacterial cell wall products such as lipopolysaccharides (LPS) [43].

Ethanol pre-exposure causes inflammatory cells of the liver, such as Kupffer cells, to release pro-inflammatory cytokines more robustly in response to a second stimulus like LPS [42]. Ethanol can also sensitize cells, causing a more robust response of cell populations downstream of cytokine inflammatory signaling. Individuals with fatty liver are LPS-induced liver injury sensitive [44].

Even in absence of infection, alcohol can alter the response to different inflammatory stimuli. Increased LPS circulation in response to alcohol consumption is due to an increase in the permeability of the gut, allowing thereby the translocation of LPS into the portal blood [45]. Experimental models showed that alcohol increased LPS permeation in both chronic and acute models [46] [47].

Another natural cause of liver injury is acetaminophen (APAP) overdose. APAP is one of the most used drugs and it is used as an analgesic or anti-pyretic drug [48]. It has been reported to be one of the most common drugs to cause drug-induced liver injury (DILI) [49]. High doses of APAP can cause acute liver injury and liver failure [50].

APAP hepatotoxicity occurs through the formation of N-acetyl-para-benzo-quinone imine (NAPQI), a highly reactive toxic metabolite, which is present in high quantities, as augmented by features of mitochondrial dysfunction, oxidative stress and glutathione (GSH) depletion leading to depletion in the store of adenosine triphosphate (ATP) [51][52][53]. Metabolic activation of APAP generates NAPQI which binds to mitochondrial proteins. Adherence to mitochondrial proteins, is important because it depletes antioxidant functions and alters the mitochondrial ATP-synthase alpha-subunit which leads to an ineffective production of ATP.

Other hepatotoxic mechanisms include toxic free radicals' formation like peroxynitrite from the reaction of nitric acid and superoxide, forming nitrotyrosine inside the mitochondria. GSH provides surplus cysteine as energy substrate for Krebs cycle. GSH also scavenges free peroxynitrite and free radicals. Mitochondria suffer damage to their own DNA by the actions of peroxynitrite compounds and reactive oxygen species [54].

APAP induces therefore cell death of hepatocytes taking on necrotic characteristic changes [55].

1.1.3.2 *Experimental systems to causes liver injury*

Liver regeneration induction by two-third hepatectomy is the most common rodent experimental model used to study liver regeneration. It was reported by Higgins et al. in 1931 and studied for decades [56]. As depicted in Figure 9, the partial hepatectomy (PHx) in rodent models involves the removal of the right and left medial, and left lateral lobes leaving the caudate and the right lateral lobes, resulting in a 66% decrease in liver size. After resection, the remaining liver tissue expands in size and proliferates to retain the original size within 5 to 7 days. In mice, the peak proliferation time is between 36 and 48 hours after PHx [57].

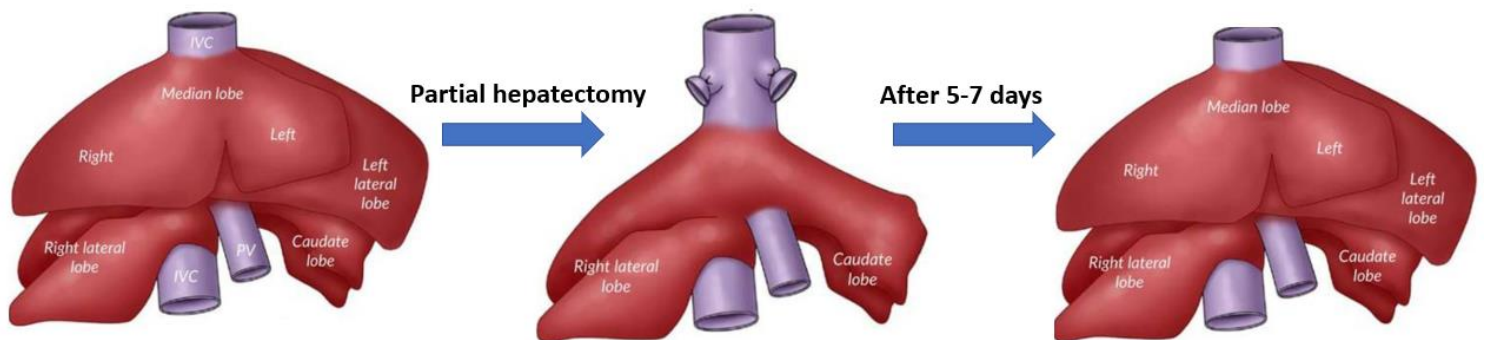


Figure 9. Partial hepatectomy in a mice liver [57].

This model is the classic and preferred model due to: (i) simple operation that does not require advanced surgical techniques, (ii) ability of the researcher to resect with a high level of accuracy because of the uniform anatomy of mouse liver, (iii) well tolerated in mice with no significant perioperative mortality, (iv) not associated with histological damage to the residual tissue, and (v) timing and accuracy of the next sequence of events that can be seen from the first minutes to 5 to 7 days. This allows PHx models to be the best choice [58].

Besides the PHx model, the liver can regenerate after a chemical-induced injury. These models are easier than PHx and has a greater clinical relevance because it induces necrotic injury as occurs in natural liver injury and disease. However, the local and systemic effects of the toxin depend on the dosage, animal species, mode of administration, nutritional status and age of the species [59].

Carbon tetrachloride (CCl_4) is one of the hepatotoxic compounds used in liver regeneration models. It induces acute liver injury after it has been broken down by cytochrome P450 2E1 (CYP2E1) leading to the formation of trichloromethylperoxy and trichloromethyl radicals, toxic and highly reactive radicals. These trigger an oxidative damage to proteins, DNA, carbohydrates, and lipids in hepatocytes causing their necrosis. It is also accompanied by KCs stimulation that produce more cytokines, free radicals, and oxygen, contributing more to cell damage. These series of events induce an acute inflammatory response represented by macrophages and leukocytes to remove hepatocytes necrotic debris. This type of injury is reversible, and it is followed by liver regeneration. It is characterized by centrilobular necrosis mainly in Zone 3 (pericentral area) where CYP2E1 is highly expressed [57] [58].

Another strong hepatotoxic compound is D-galactosamine. This compound disturbs the metabolic system in the liver causing an acute liver failure and leading to the depletion of uridine triphosphate and therefore, inhibition of protein and RNA synthesis. D-galactosamine contributes as well to the necrosis and inflammation of the liver by promoting the degranulation of the intestinal mast cell that represents the intestinal barrier, thus allowing endotoxins to

reach the liver's portal circulation. The capacity of liver regeneration in this model is weaker than that of the CCl₄ model [56] [57] [59].

1.1.3.3 Pathways of liver regeneration after PHx

The processes leading to liver regeneration following partial hepatectomy are enlargement of hepatocytes (compensatory hypertrophy) followed by proliferation of hepatocytes (hyperplasia).

PHx leads to the proliferation of all cell populations within the liver, including biliary epithelial cells, endothelial cells, and hepatocytes. Within 10 to 12 hours after a surgery DNA synthesis is initiated and ceases in about three days. Cellular proliferation begins around the portal triads (periportal region) and continues towards the center of the lobules. Hepatocytes proliferating form clumps soon transformed to classical plates. Proliferating endothelial cells develop to fenestrated cells like the ones found in the sinusoids [60].

Changes in gene expression due to regeneration can be observed within minutes after an hepatic resection. A number of transcription factors are induced and participate in orchestrating the expression of a group of hepatic mitogens. Hepatocytes proliferating appear to revert, partially, to a fetal phenotype and to express markers like alpha-fetoprotein. Regenerating hepatocytes continue to conduct normal metabolic functions like support of glucose metabolism [60].

Three phases have been described in the process of liver regeneration: (i) Priming or initiation phase, (ii) proliferation phase, (iii) terminal phase. Figure 10 shows the sequence of events following partial hepatectomy.

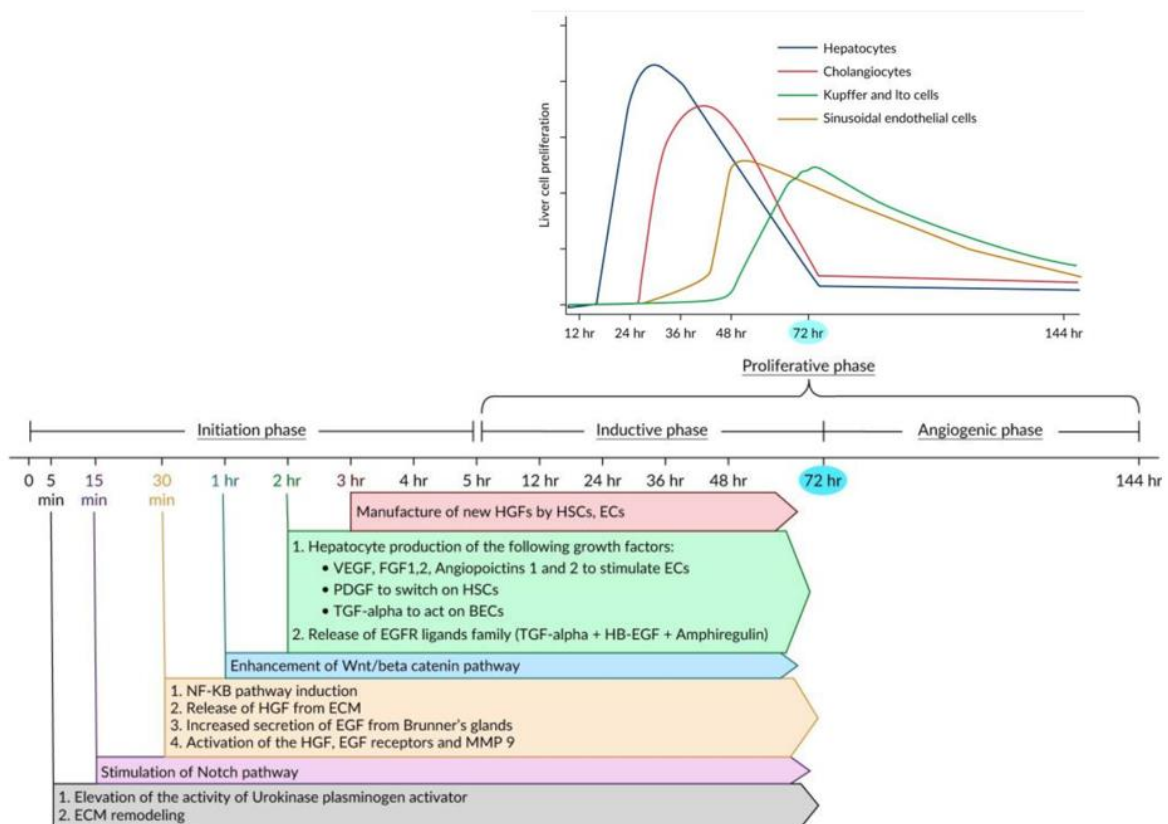


Figure 10. Temporal sequence of events after a partial hepatectomy [56].

1.1.3.3.1 Priming or initiation phase

Priming or initiation phase occurs in the first 0-5 hours after PHx [58]. These events are mediated by growth factors and cytokines and modify multiple genes expression to prepare the re-entry of the liver cells into the cell cycle. After a PHx, more than 100 genes become activated during this priming phase. Hemodynamic changes after PHx have been shown to be necessary for starting liver regeneration after PHx [58]. These changes have been observed to be restricted to portal blood flow with no effect on the arterial part. PHx causes an increase in the contribution of portal blood flow resulting in an increase in growth factors and cytokines from the pancreas and intestine per hepatocyte [58]. Additionally, there is a mechanical stress on endothelial cells caused by a rise in portal blood pressure. This is due to the portal blood flow having to pass through capillary beds which have a cross sectional area that is around one-third smaller than normal liver. Sokabe et al. documented in 2004 that these endothelial cells express an increased activity of urokinase plasminogen activator (uPA) following mechanical stress [61].

The rise of uPA can be observed 5 minutes after PHx. Within 10 minutes, it converts plasminogen into plasma which breaks down fibrinogen into fibrinogen degradation products (FDPs). At 30 minutes and until 24-48 hours after PHx, plasmin increases the transformation

of pro-matrix metalloproteinases (pro-MMPs) into MMPs. Both plasmin and MMPs are involved in the turnover and remodeling of many extracellular matrix (ECM) proteins [62]. During matrix remodeling, an hepatic growth factor (HGF) in its inactive form is attached to the ECM and it is activated by uPA and excreted systemically and locally causing the activation of the HGF receptor (HGFR or c-Met) 30 minutes to 1 hour after PHx. At the same time, an epidermal growth factor (EGF) produced by the duodenum, stimulates an EGF receptor (EGFR) [63]. Several studies have proven that there is a cross interaction between EGFR in which the activation of c-Met increases EGFR activity [64].

1.1.3.3.2 NF-KB signaling pathway

Role of innate immunity components

Innate immunity is the main stimulation for liver regeneration initiation [65]. After PHx, innate immunity is activated and the production of its components such as complements (C3a and C5a) and lipopoly-saccharides (LPS) is initiated. Complement proteins (C3a and C5a) and LPS bind to their respective receptor, complement receptors and Toll-like receptor 4, on KCs surface [65]. These interactions lead to the activation of a signaling pathway known as the nuclear factor kappa B (NF-KB) pathway. The most common NF-KB is made by the combination of P65 and P50. Under normal conditions, NF-KB is inside the cytoplasm of KCs by inhibitory KB protein (IKB). When extracellular signals like C5a, C3a and LPS stimulate KCs, IKB undergoes degradation and phosphorylation by IKB kinase, allowing NF-KB to become free and therefore move into the nucleus where it will excite the transcription of cyclin D1, tumor necrosis factor (TNF) and interleukin 6 (IL6) [58]. This process occurs within the first hour after PHx.

IL6 is responsible for the activation of about 40% of the genes, not expressed in normal liver, that are expressed and triggered in the remaining tissue after PHx [66].

Role of tumor necrosis factor alpha (TNFa)

TNFa has a vital role in the priming phase through two important functions: (i) activation of NF-KB signaling pathway by binding to KCs TNF receptor 1 creating a cycle, and through the indirect induction of the inhibitory KB kinase (IKK) [67] [68], (ii) stimulation of stress-activated protein kinase (SAPK), also known as c-Jun N-terminal kinase (JNK), in hepatocytes.

JNKs are special kinase proteins that enhance liver regeneration. They are activated by mitogen-activated protein kinase kinases or SAPK/extracellular signal-regulated kinase kinases, SEK2/MKK7 and SEK1/MKK4 [67]. These kinases are triggered as a response to PHx leading to the activation of JNK which phosphorylates c-Jun TF in the nucleus to induce

cyclin-dependent kinase 1 (CDK-1) transcription, resulting in the proliferation of hepatocytes [65] [67][68].

1.1.3.3.3 Wnt/beta catenin signaling pathway

Within 1 to 3 hours after PHx, Wnt/beta catenin signaling pathway starts to operate. This pathway is launched by the binding of the secreted TNF α to its specific receptors on HSCs, sinusoidal endothelial cells and KCs, releasing Wnt ligands, specific glycoproteins [69]. Furthermore, neither hepatocytes nor biliary epithelial cells secrete Wnt ligands after PHx, thus Wnt proteins have to undergo palmitoylation and glycosylation by the porcupine enzyme which is found in the endoplasmic reticulum [69]. Following this, the cargo receptor protein Wntless (Wls) transfers Wnt proteins to the cell membrane from the Golgi apparatus, for extracellular secretion [70]. The active Wnt protein that has been released binds to its Frizzled receptor associated with a co-receptor on hepatocytes in order to mediate the activation of Wnt/beta catenin signaling pathway by sending an inactivating signal to beta-catenin degradation complex (B-CDC) that consists of casein kinase 1 (CK1), adenomatous polyposis coli gene product, axin and glycogen synthase kinase 3 β to stop the phosphorylation of Wnt proteins [71]. This interaction allows Wnt proteins to be released from B-CDC and translocated to the nucleus to be able to combine with the lymphoid and T-cell enhancing transcription factors that induce target genes, like cyclin D1, transcription that play a role in the proliferation of hepatocytes [69][72].

1.1.3.3.4 Notch signaling pathway

The notch signaling pathway is one of the first pathways to be turned on after PHx (within 15-30 minutes). This pathway is dependent on two proteins, NOTCH-1 receptor and NOTCH-1 ligand, also known as JAGGED-1, proteins which are upregulated 1 to 5 days following PHx [73][74]. In normal liver there are four different NOTCH receptors expressed on cholangiocytes, hepatocytes, endothelial cells lining the sinusoids and portal vessels, and hepatic progenitor cells (HPC). They are stimulated by the interaction with their specific membrane-bound ligand proteins: (i) Delta-like 1, 3, and 4 (DLL 1,3,4), and (ii) Jagged-1 and -2 [75][76]. However, DLL4 and Jag-1 are the only NOTCH ligands present in human liver. Jag-1 is expressed in smooth muscle cells in the mesenchyme of the portal vein, and in biliary cells, HPCs [73]. After liver injury, a cell-cell interaction between cells that express JAG ligands and cells that carry NOTCH receptors causes NOTCH receptors activation by JAG ligands, which leads to a Notch intracellular domain formation in the cytoplasm. The Notch signaling pathway is important for the regeneration of the vasculature of the liver [77].

1.1.3.3.5 Proliferation phase

This phase is divided into 2 main periods:

- (i) Induction phase: proliferation of hepatocytes and cholangiocytes. Hepatocytes regenerative response precedes and triggers cholangiocytes expansion. This step initiates at the end of the initial or priming phase and lasts for 72 hours reaching its peak at 24-36 hours after PHx [58].
- (ii) Angiogenic phase: nonparenchymal cells such as KCs, hepatic endothelial cells and HSCs undergo proliferation in response to proliferating hepatocytes signals. This phase occurs after the inductive phase and continues for 2 or 3 days [58].

All the cells undergo firstly cellular hypertrophy followed then by cellular proliferation.

1.1.3.3.6 Termination phase

Following the proliferation phase, remnant tissue expands and retrieves original size correspondent to the normal liver. The primary mechanism of this process is represented by the autonomic hepatocyte proliferative capacity. Still, this characteristic can continue working and giving liver cells which in severe cases can lead to carcinogenesis. This is why the liver must undergo a termination phase controlled by proliferative inhibiting factors that act as brakes to constrain liver cell proliferation, correct a regenerative response overshooting and prevent carcinogenesis of the excess proliferating cells [78].

Transforming growth factor β (TGF- β)

Transforming growth factor β (TGF- β) most popular anti-proliferative factor that can stop the liver regeneration process. TGF- β is secreted, mainly, by nonparenchymal cells such as KCs, platelets, and HSCs [78].

Pericellular hepatic ECM is formed by 2 important components called decorin, attached to pro-TGF β and glycosaminoglycan, bound to HGF. As already described, urokinase is activated early after PHx leading to the degradation of the ECM and the release of certain GF through integrin signaling pathway. TGF- β levels increase at 3 hours reaching its peak at 72 hours after PHx. Urokinase activity transforms HGF to its active form, while pro-TGF β is neutralized by α -2-macroglobulin in blood plasma blocking its activity and hanging the net balance of HGF from the priming phase [79].

Halfway through the proliferation phase, an indirect inhibitor of hepatocyte growth, cation-independent mannose 6-phosphate receptor (CIMPR) is induced causing the conversion of pro-TGF β into the active form of TGF- β . It also mediates the interaction between the active

form of TGF- β and its specific receptors on hepatocytes, terminating this way the mitotic response after the complete expansion of liver cells [80].

Several mechanisms have been proposed to describe how liver regeneration is stopped by TGF- β .

Firstly, the binding of TGF- β to TGFR results in the receptor-regulated cytoplasmic phosphorylation against decapentaplegic (R-Smad) proteins that are later translocated into the nucleus. Once in the nucleus, they stimulate the expression of CDK inhibitors, cell cycle inhibitors, and suppress the production of cyclins D and E, and CDKs 2 and 4 (cell cycle inducers), leading to cell cycle arrest at G1/S transition [80].

Secondly, TGF- β 1 starts the remodeling of the hepatic lobes and corrects the proliferation overshooting by inducing apoptosis of excess hepatocytes releasing reactive oxygen species (ROS) through the c-Jun-independent mechanism [81].

1.2 Actual regenerative theories

Although the turnover of parenchymal cells from the liver is slow, this organ displays a high regenerative capacity being able to restore 70% of the lost tissue within a few weeks [2]. The ability of the liver to be capable of maintaining a constant mass is critical for the survival of organisms. For liver injuries ranging from mild to extreme, differentiated hepatocytes re-enter the cell cycle, proliferate and replenish the lost tissue.

In 2015, it was stated by Wang et al. that a population of proliferating and self-renewing pericentral hepatocytes, adjacent to the central vein in the lobule, was identified by lineage tracing using Axin2 (Wnt-responsive gene) in mice. These cells expressed the progenitor marker Tbx3 and were diploid, thereby differing from mature hepatocytes which tend to be polyploid. Pericentral cells descendants differentiated into polyploid hepatocytes (Tbx3-negative) and could replace all hepatocytes along the liver lobule during homeostasis. Lastly, endothelial cells adjacent to the central vein provided Wnt signals that maintain the pericentral cells constituting this way the niche [28]. However, it has been demonstrated by Sun et al. in 2020 that there is an equitable reparative and homeostatic potential of all hepatocytes, regardless of their ploidy status or lobular location. Sun et al. stated that Axin2⁺ pericentral hepatocytes have limited contribution to liver regeneration and homeostasis [82].

Chow et al. demonstrated in 2019 that Lgr5⁺ expression in the liver was restricted to a unique hepatocyte subset adjacent to central veins. By genetic lineage tracing, they were able to see that Lgr5⁺ pericentral hepatocytes contribute, mainly, to their own lineage preservation

during postnatal liver homeostasis and development. These hepatocytes also sustain their own lineage regeneration during the rapid and massive regeneration process after a two-thirds PHx. Additionally, Lgr5+ hepatocytes were found to be the principal cellular genesis of diethylnitrosamine (DEN)-induced hepatocellular carcinoma (HCC). These findings established an unexpected self-maintaining model for a specific subset of hepatocytes during regeneration and homeostasis of the liver, and identified Lgr5+ pericentral hepatocytes as the major cells of genesis in HCC development [83].

1.3 Workflow

1.3.1 Characterizing the location of hepatocyte proliferation and death

In order to understand the extent and location of hepatocyte turnover in terms of both cell death and cell proliferation, we will analyze uninjured livers from both humans and mice. To improve this understanding, we will immunostain thick slices to identify the proliferative hepatocytes, using (i) an antibody for Ki-67, (ii) antibody for glutamine synthetase to identify pericentral hepatocytes, and (iii) an antibody for cytokeratin 19 to identify the portal tracts. This combination of stains will help us identify dying and proliferating hepatocytes as well as the location of these cells with respect to the portal and central veins. We will image the slices by confocal microscopy and then quantify the percent of apoptotic and proliferative hepatocytes in each liver lobule zone.

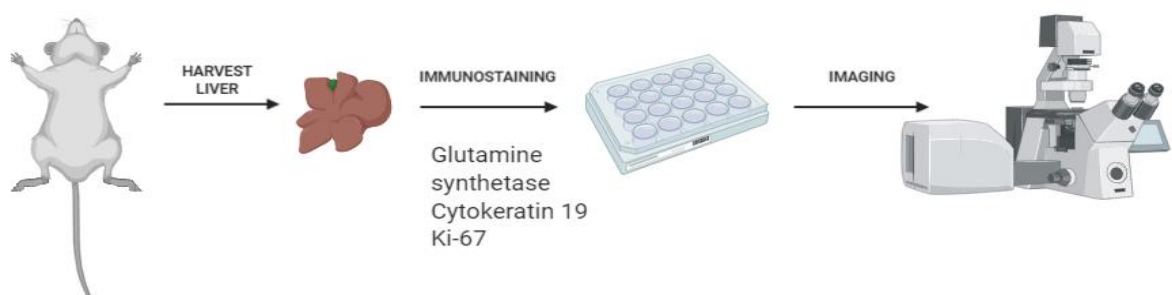


Figure 11. simplified overview of the experiment that will be conducted.

1.3.2 Trace the fate of proliferative hepatocytes

To see how proliferative hepatocytes contribute to hepatocyte turnover, we will employ an unbiased lineage tracing strategy. We will mate a mouse harboring a tdTomato reporter to a Ki67CreER mice, so that in the presence of tamoxifen, proliferative cells will become tdTomato-positive. A single dose of tamoxifen will be injected into the Ki67CreER;tdTomato mice to label all proliferating hepatocytes within a day of the tamoxifen injection. We will then keep these mice alive for 1 month at which we will harvest their livers, stain them, and image them by confocal microscopy. This way, we will determine how proliferative hepatocytes contribute to hepatocytes along the liver lobule.

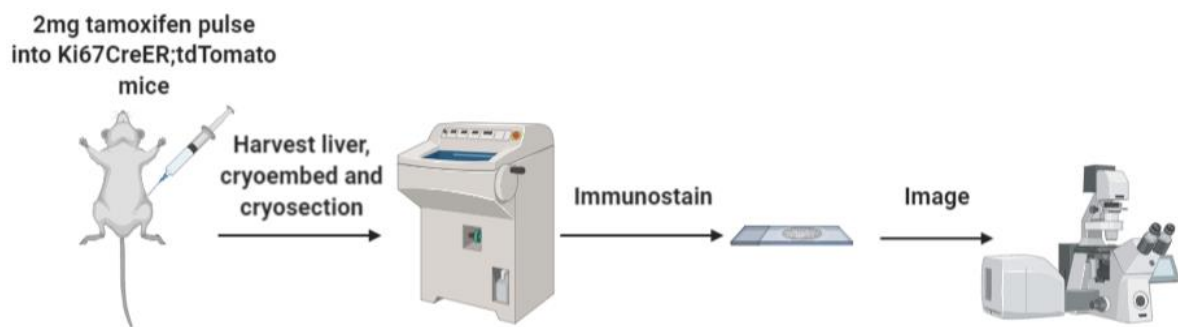


Figure 12. Simplified overview of the experiment that will be conducted.

1.4 Aim of the project

The main goal of this project is to be able to understand the behaviors and pathways that hepatocytes engage to be able to regenerate the liver. This project will study two different steps. Firstly, immunofluorescence, tissue processing and imaging will be used to study if there is any subset of hepatocytes with an increased proliferative capacity by using specific antibodies like Ki-67. Secondly, lineage tracing will be performed to determine how the different proliferative hepatocytes contribute to the liver hepatocyte population.

2 Methodological considerations

2.1 Used antibodies

Ki-67 is expressed by cells that are actively progressing through the cell cycle and not by quiescent cells [84]. The expression of Ki-67 is associated with tumor cell proliferation and growth and it is used as a proliferation marker as well as in immunohistochemistry [85]. During interphase, the Ki-67 antigen is detected exclusively within the nucleus, while during mitosis most of Ki-67 is relocated to the surface of the chromosome [86]. Ki-67 is an excellent marker to identify proliferative cells in a large cell population. In this project, the Ki-67 antibody will be used to identify proliferative hepatocytes in uninjured livers from both humans and mice.

Glutamine synthetase (GS) is an antibody that marks pericentral hepatocytes and thereby reveals the location of the central veins (Figure 11).

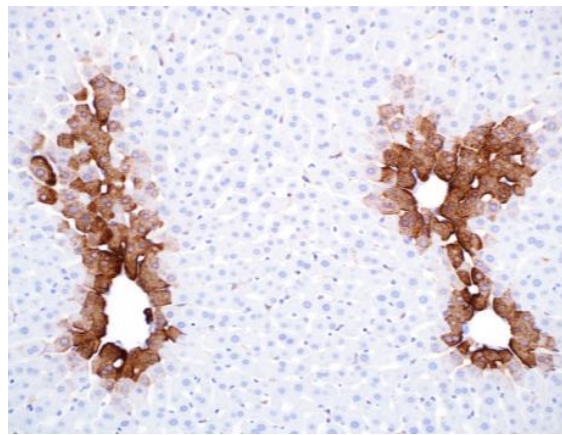


Figure 13. Staining of pericentral hepatocytes revealing the central veins [87].

Cytokeratin 19 (CK-19) is an antibody that marks bile ducts and thereby reveals the location of the portal tracts (Figure 12).

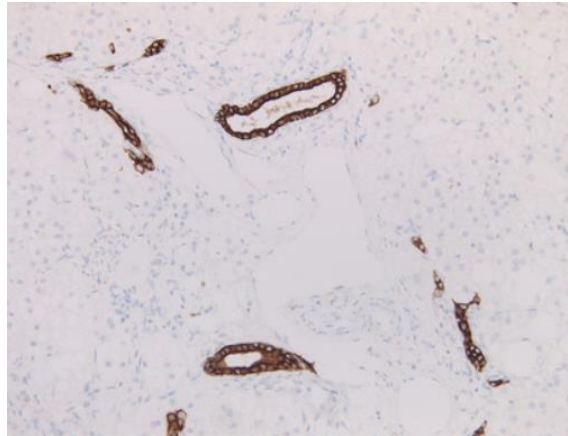


Figure 14. Staining of bile ducts revealing the location of the portal tracts.

2.2 Lineage tracing

Lineage tracing encompasses various methods that enable tracking the fate of individual cells and their progeny with minimal disturbance of their physiological function. It has been used to define complex biological processes involving cell types with different lineage hierarchies.

Lineage tracing also allows specificity of labeling. For example, Cre-lox recombination is a site-specific recombinase technology used for lineage tracing. It involves the targeting of a DNA specific sequence and the splicing of it using the Cre recombinase. This system is used as a genetic tool to control recombination events in genomic DNA. It has allowed researchers to manipulate several genetically modified organisms to be able to control gene expression, modify the architecture of desired chromosomes and delete undesired DNA sequences [88][89]. The Cre-loxP site-specific recombination system has risen as an important tool for conditional somatic mouse mutant's generation. This method allows the control of gene activity in time and space in almost every tissue of the mouse used in the study of gene function and establishing animal models for human disease. The temporal regulation of Cre in the cell population can be obtained by a small molecule inducer through the fusion of Cre and a ligand-binding domain of steroid receptors. One of these ligand-dependent receptors is the CreER recombinase which is inactive but can be activated by using tamoxifen, a synthetic estrogen receptor ligand [90].

Following tamoxifen administration, the CreER recombinase is able to remove LoxP-STOP-LoxP cassette to allow expression of a colorimetric or fluorescent protein to label the cell and its progeny at the genetic level [91].

3 Methods

3.1 Previous findings methods

3.1.1 Self-renewing diploid Axin2⁺ cells fuel homeostatic renewal of the liver

3.1.1.1 *Animals*

Axin2-CreERT2;Rosa26-mTmGflox mice were obtained from the Jackson Laboratory.

3.1.1.2 *Lineage tracing*

For lineage tracing experiments, Axin2-CreERT2;Rosa26-mTmGflox mice (8-12 weeks old) received intraperitoneal tamoxifen injections. The concentration of tamoxifen per injection was of 4mg per 25g mouse weight dissolved in 10% corn oil/ethanol on five consecutive days.

3.1.1.3 *Liver immunofluorescence and histology*

Mouse livers were fixed overnight at 4°C in 4% PFA, cryoprotected in 30% sucrose at 4°C for 24 hours then embedded in OCT and snap frozen. Cryosections were 10 µm thick and were incubated in blocking buffer at room temperature. They were then stained with primary and secondary antibodies and the slides were mounted using Prolong Gold with DAPI mounting medium.

3.1.1.4 *Hepatocyte proliferation assay*

Hepatocyte proliferation was measured in vivo by 5-ethynyl-2'-deoxyuridine (EdU) uptake. For this, mice received a dose of EdU intraperitoneally (50 mg per kg) daily for seven days and harvested half a day after the last EdU injection. For the detection of EdU, cryosections were stained with primary and secondary antibodies and then incubated.

3.1.1.5 *Hepatocyte ploidy measurement*

FVB mice were used for hepatocyte ploidy measurements. For the measurement of ploidy of Axin2⁺ hepatocytes, Axin2-CreERT2;Rosa26-mTmGflox mice were injected five daily doses of tamoxifen, 4mg per 25 g of body weight, and cells were then isolated either two days or one year after the last pulse of tamoxifen and were then stained with Hoechst 33342. After this, cells were analyzed using the FACS ARIA II machine and data was processed with FlowJo v10 FACS plots and FACSDiva 8.0 software.

3.1.2 Lgr5⁺ pericentral hepatocytes are self-maintained in liver homeostasis

3.1.2.1 Animals

Lgr5-rtTA/TetO-Cre/R26-tdTomato mice was generated in the Walter and Eliza Hall Institute of Medical Research animal facility in Australia.

Only male mice were used for the DEN-induced liver tumor experiment. A mix of both females and males were used in the rest of the experiments and no gender-bias was observed.

3.1.2.2 Liver injury models

A PHx was performed to induce injury. Eight to twelve weeks old Lgr5-rtTA/TetO-Cre/R26-tdTomato mice were pulsed with doxycycline feed for seven days and back to normal food for seven more days before surgery. Mice were anesthetized with oxygen and 2% isoflurane flow in a Plexiglas chamber and then were transferred to a Styrofoam pad. Anesthesia was maintained throughout the entire procedure through inhalation using a mouthpiece. Abdominal fur was removed, and the abdominal skin was disinfected with ethanol 70%. A mid-line skin and muscle incision was then performed to expose the internal abdominal cavity and therefore the liver. For the ligation of the left lateral liver lobe and middle lobe, a 4-0 silk thread was used and the lobes were resected just above the knots. After the PHx, the peritoneum and skin were closed with 5-0 suture and the mouse was placed in an individual cage under a warming pad for recovery. Regenerating livers were then harvested two weeks after the PHx surgery was performed.

For the DEN-induced liver injury, male mice at 12 days postnatal were injected intraperitoneally with a single dose of DEN, 25mg per kg of mouse weight, in sterile PBS. Mice were raised after the DEN injection and were euthanized once tumors started to be detected.

3.2 Actual project methods

3.2.1 Creating liver tissue samples

In order to create new samples to be able to proceed with the next experiments, the mouse breed has to be decided. In this case, C57BL/6J mice were used.

Different parameters should be taken into consideration such as age, and gender. In this case, 4 mice were used. These mice were 8 weeks old and two of them were females and two were males.

To be able to harvest their livers, they will first have to be anesthetized. At the Whitehead Institute for Biomedical Research the anesthesia that is used for this purpose is isoflurane.

The set up and perfusion system used is depict in Figure 15 and Figure 16. The mouse is first anesthetized by introducing it in the glass box (Figure 15, (1)) which is infused with the anesthetic (Figure 15 (2)). Once the mouse is anesthetized, it is transferred to the surgical table (Figure 16 (1)) were it will get more anesthesia, until the end of the procedure, through a nose cone Figure 16 (2)). An incision will be made through the abdominal cavity Figure 16 (3) to expose the liver and other vital organs. Once the liver is exposed, a needle, connected to the perfusion system Figure 16 (4)), will be introduced into the hepatic vein to perfuse the mouse liver with firstly 30 mL of PBS to clear blood from the organ, and secondly with 30 mL of 4% para-formaldehyde (PFA) in PBS with 0.1% Tween-20 to fix the organ. The perfusion system and pump used is depict in Figure 15 (3). Once this is completed, the liver will be harvested and submerged in 4% PFA in PBS with 0.1% Tween-20 and stored at 4°C over-night to let it fix further. After harvesting their liver, the mice are kept in trash bags and taken to the animal facility to be taken care of. Table 1 shows a summary of the mice used, their age, gender, treatment, fixation, and label.



Figure 15. setup of the perfusion system used during the experiment.

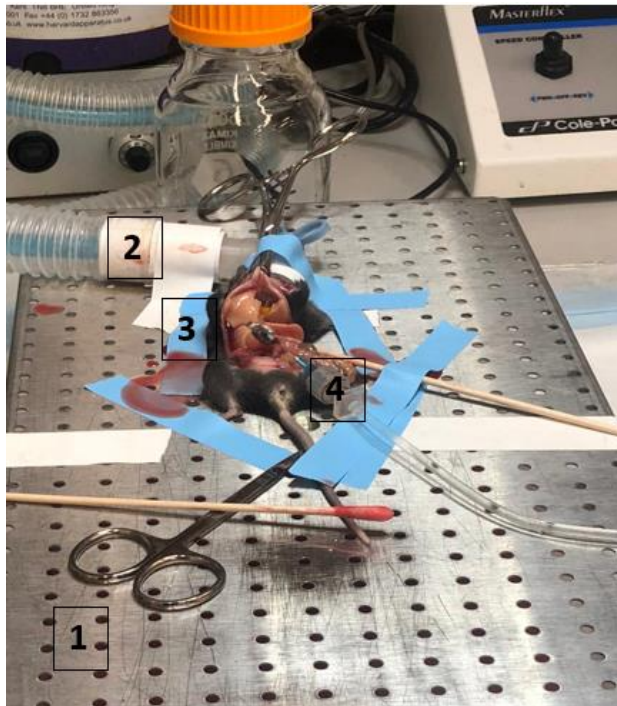


Figure 16. Surgical procedure performed to perfuse and harvest liver tissue.

Table 1. Summary of the different characteristics of the mice used for this experiment.

| Label given | Age | Gender | Treatment | Fixation |
|-------------|---------|--------|-----------|--|
| ED2T | 8 weeks | Male | None | PBS Perfusion, PFA + 0.1% Tween-20 Per- fusion, PFA + 0.1% Tween-20 overnight |
| ED3T | 8 weeks | Male | None | PBS Perfusion, PFA + 0.1% Tween-20 Per- fusion, PFA + 0.1% Tween-20 overnight |
| ED4T | 8 weeks | Female | None | PBS Perfusion, PFA + 0.1% Tween-20 Per- fusion, PFA + 0.1% Tween-20 overnight |
| ED5T | 8 weeks | Female | None | PBS Perfusion, PFA + 0.1% Tween-20 Per- fusion, PFA + 0.1% Tween-20 overnight |

3.2.2 Locating proliferative hepatocytes in thick liver tissue

After the liver samples had been fixed overnight, the tissue was washed with PBS for 5 minutes three times in total. Two slices of 1 mm thickness, from each liver that was harvested, were taken. The rest of the tissue was stored in 10 mL PBS with 40 μ L 5% NaN₃ at 4°C.

After the 1mm tissue samples were cut, sodium citrate antigen retrieval was performed for 20 minutes using a pressure cooker. The need for antigen retrieval depends on several variables including the type of tissue, duration and method of fixation and the target antigen. Performing the antigen retrieval technique in the pressure cooker, reverses some of the chemical cross-links caused by fixation and allows the restoration of tertiary or secondary structures of the epitope. The sodium citrate antigen retrieval buffer was prepared following the recipe from the protocol “Immunostaining and clearing tissue slices” found in the appendix.

The samples were then washed with PBS and placed in a 24 well plate as depict in Figure 17. The slices were then permeabilized with 0.5% Triton X-100 in PBS at room temperature for 1 hour. After this, the primary antibodies listed in table 2 were diluted in Tx buffer, added to the tissue, and incubated at 37°C with shaking for 48 hours. After those 48 hours, the tissue slices were washed with Tx buffer at room temperature 3 times for 30 minutes each. After that, the secondary antibodies listed in table 2 were diluted in Tx buffer, added to the tissue, and incubated at 37°C with shaking for 48 hours. The slices were then washed with Tx buffer three times for 30 minutes each and they were then incubated overnight with shaking in clearing-enhanced 3D (Ce3D) solution and then were imaged using the Zeiss 710 confocal microscope.

This tissue slices were stained for Actin FITC, glutamine synthetase-568, Ki67 and CK-19 (Table 2).

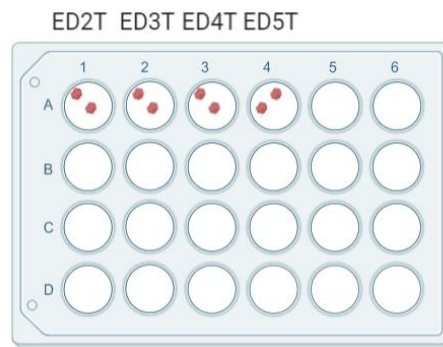


Figure 17. Display of the tissue samples in a 24 well plate.

Table 2. Primary and secondary antibodies used to immunostain tissue samples.

| Primary Antibodies | | Secondary Antibodies | |
|--------------------|-------------|----------------------|-------------|
| Actin FITC | 1 μ L | Anti-Rb 568 | 0.5 μ L |
| Ms anti-GS-568 | 1 μ L | Anti-Rt 647 | 0.5 μ L |
| Rb anti-CK19 | 5 μ L | Block | 500 μ L |
| Rt anti-Ki67 | 2.5 μ L | | |
| Block | 500 μ L | | |

3.2.3 Lineage tracing of proliferative hepatocytes

To test whether some hepatocytes tend to proliferate more than others, the following experiment was conducted: a male and female Ki67CreER;tdTomato mouse were given 2mg tamoxifen injections every other day for one month. These mice continue to live for another two weeks, to let all tamoxifen wash out of the system and prevent any new proliferative cells from being labeled. After those two weeks, the livers were harvested and fixed. If it is true that there are some hepatocytes that are more likely to proliferate, then the cells that are actively proliferating at the time of harvest should be more likely to have proliferated in that prior month of labeling.

Tissue samples were cryoembedded, using an optimal cutting temperature (OCT) compound, in two different blocks. Once the tissues were cryoembedded, two 12 μ m thick slices of each sample were cut using a LEICA CM3050 S cryostat and placed in a Fisherbrand Superfrost plus microscope slide (precleaned) from Fisher scientific, as shown in Figure 18.

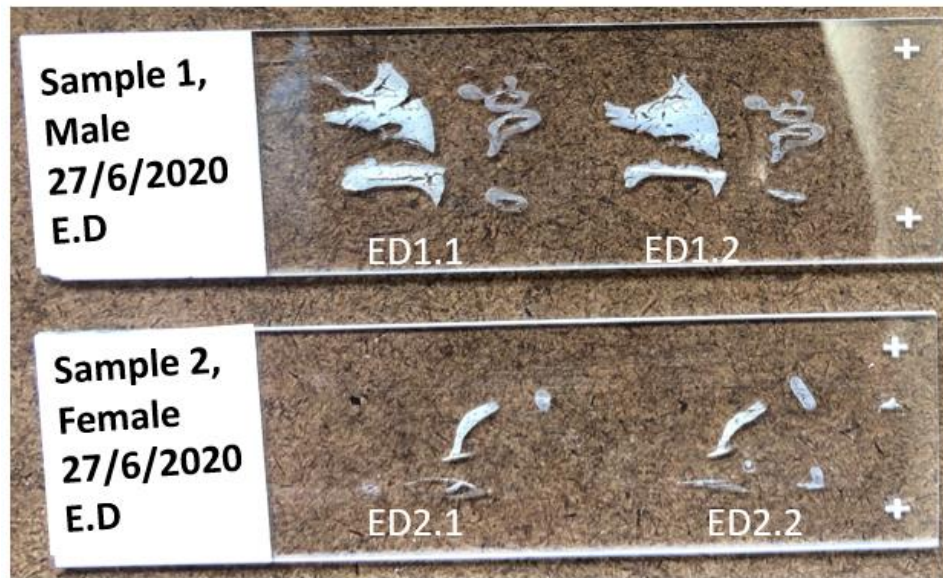


Figure 18. display of the cryosectioned liver tissue from both liver samples. Sample 1 corresponds to the liver tissue from the male Ki67CreER;tdTomato mouse and sample 2 corresponds to the female Ki67CreER;tdTomato mouse.

Once the samples were cryosectioned, the sections were immunostained following the “immunostaining cryosections” protocol, found in the appendix section, staining for different antibodies as listed in Table 3 and Table 4 and finally, imaged using the Zeiss 710 confocal microscope.

Table 3. List of primary and secondary antibodies used to immunostain samples ED1.1 and ED2.1.

| Primary Antibodies | | Secondary Antibodies | |
|--------------------|-------------|----------------------|-------------|
| Gt tdTomato | 1 μ L | Anti-Gt 488 | 0.5 μ L |
| Rt anti-Ki67 | 2.5 μ L | Anti-Rt 647 | 0.5 μ L |
| Actin-405 | 2 μ L | Block | 500 μ L |
| Ms anti-GS-568 | 1 μ L | | |
| Block | 500 μ L | | |

Table 4. list of primary and secondary antibodies used to immunostain samples ED1.2 and ED2.2.

| Primary Antibodies | | Secondary Antibodies | |
|--------------------|-------------|----------------------|-------------|
| Gt tdTomato | 1 μ L | Anti-Gt 568 | 0.5 μ L |
| Rt anti-Ki67 | 2.5 μ L | Anti-Rt 647 | 0.5 μ L |
| Actin-405 | 2 μ L | Anti-Rb 488 | 0.5 μ L |
| Rb anti-CK-19 | 5 μ L | Block | 500 μ L |
| Block | 500 μ L | | |

4 Results

4.1 Previous findings

4.1.1 Self-renewing diploid Axin2⁺ cells fuel homeostatic renewal of the liver

4.1.1.1 Axin2⁺ cells self-renew

One of the defining properties of stem cells is their ability to self-renew. To test of Axin2⁺ cells self-renew, Wang et al. administered mice with tamoxifen in five consecutive doses (Figure 19a). Over time, labelled cells expanded concentrically from the central vein and all pericentral cells remained labelled (Figure 19b, c). Figure 19c also shows that while Axin2⁺ cells can produce all hepatocytes along the lobule (Figure 19c), they are not replaced by Axin2⁻ unlabeled cells showing then that pericentral Axin2⁺ cells conform a self-renewing cell population.

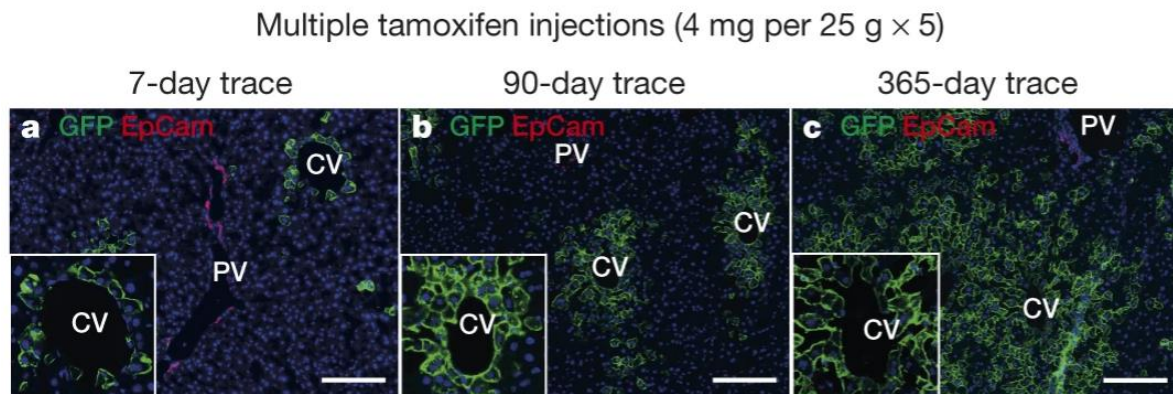


Figure 19. Axin 2⁺ cells self-renew. A) Pericentral hepatocytes labelled in Axin2-CreERT2;Rosa26-mTmGflox mice after the administration of five consecutive doses of tamoxifen. Traced for 7 days. B) After 90 days of tracing. And C) after 365 days of tracing, show that all pericentral hepatocytes remained labelled. (Figure edited from [28])

4.1.1.2 Axin2⁺ cells proliferate faster than other hepatocytes

The fact that Axin2⁺ cells repopulate most of the liver lobule means that the rate of proliferation of Axin2⁺ cells is greater than the rate of proliferation of Axin2⁻ cells. To demonstrate this, Wang et al. quantified the DNA synthesis rate of both cell populations. Five Axin2-CreERT2;R26-mTmGflox mice were labelled with tamoxifen and after that they were given seven daily doses of EdU (Figure 20).

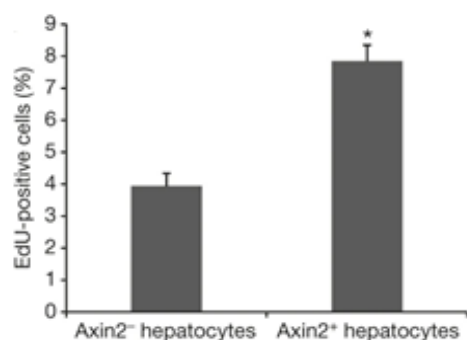


Figure 20. Axin2⁺ cells proliferate faster than other hepatocytes. The image shows the quantification of EdU⁺ cells within Axin⁺ and Axin⁻ hepatocyte populations. N=5 mice. (Figure edited from [28])

4.1.1.3 Axin2⁺ cells are mostly diploid

Most of mature hepatocytes are polyploid, characteristic that is associated with an increase in senescence and a decreased proliferative potential [92][93]. Generally, stem cells are diploid, a necessary property for unlimited duplication [94][95]. To be able to isolate the Axin2⁺ cells and evaluate whether they are polyploid cells, Wang et al. used FACS sorting with Hoechst 33342 staining. As depicted in Figure 21a and c (left bar), the majority of unsorted hepatocytes are polyploid cells. In comparison, the majority of Axin2⁺ turned out to be diploid (Figure 21 b and c (middle bar)). To confirm whether diploid Axin2⁺ cells give rise to polyploid cells, they labelled Axin2⁺ cells with tamoxifen and traced them for one year. After that year of tracing, they isolated GFP⁺ cells for ploidy analysis. They found out that after a year of tracing the ploidy distribution of GFP⁺ cells were the same as that of unsorted hepatocytes, suggesting this way that after leaving the pericentral zone, Axin2⁺ descendant cells mature into polyploid cells. This is shown in Figure 21 c (right bar).

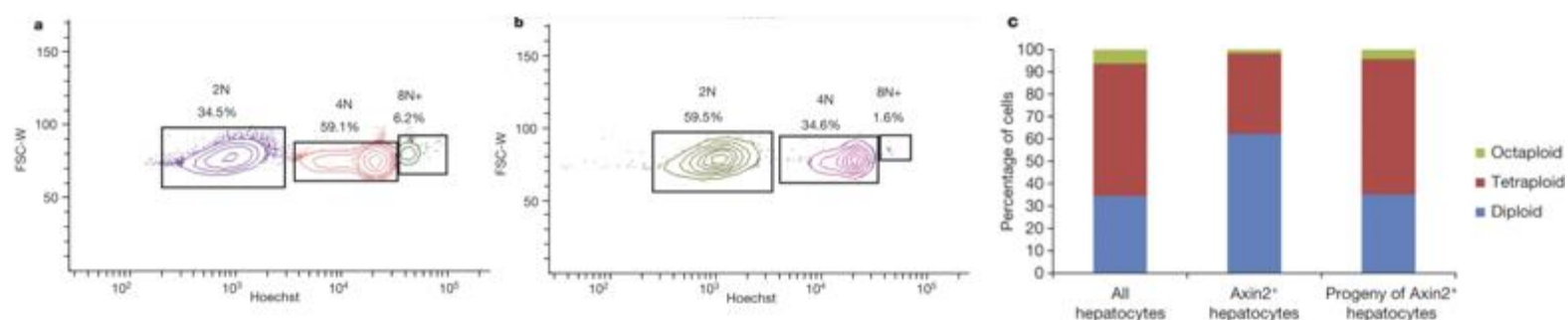


Figure 21. Axin2⁺ cells are mostly diploid. A) FACS plot of all hepatocytes stained with Hoechst 33342. Gated for 2N (diploid), 4N (tetraploid) and 8N+ (octaploid or more) cells. B) FACS plot of Axin2⁺ cells stained with Hoechst 33342. Gated the same way as in A. C) Ploidy distribution: unsorted hepatocyte population on the left, Axin2⁺ hepatocyte population on the middle and labelled hepatocytes after lineage tracing for 1 year on the right. N=3 mice per group. (Figure edited from [28])

4.1.2 Lgr5⁺ pericentral hepatocytes are self-maintained in liver homeostasis

4.1.2.1 Lgr5⁺ hepatocytes generate their own lineage during liver regeneration upon PHx

As shown in Figure 22, the harvested liver lobules of Lgr5-rtTA/TetO-Cre/R26-tdTomato mice 14 days postsurgery, showed similar tdTomato patterns in unoperated and regenerated liver lobes of age-matched mice while the size increase of the lobe showed a significant liver growth.

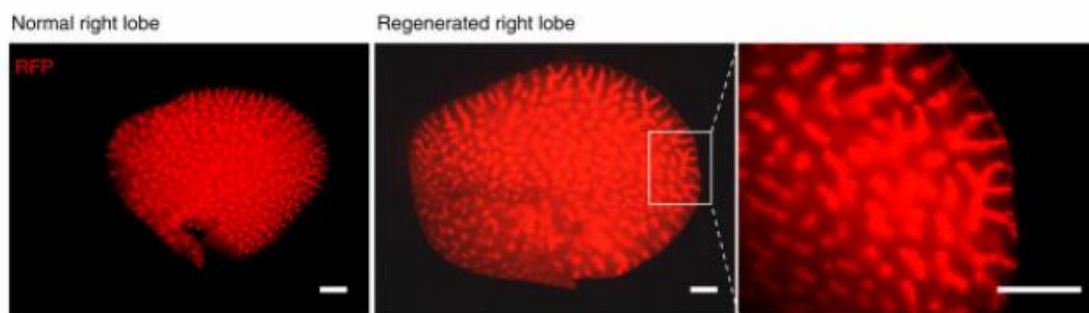


Figure 22. experimental strategy for PHx experiments performed on Lgr5-rtTA/TetO-Cre/R26-tdTomato mice. Images represent the right liver lobe adult control and Lgr5-rtTA/TetO-Cre/R26-tdTomato mice harvested 14 days after PHx. N=5 mice. (Figure edited from [83]).

Immunostaining on sections of the regenerated liver lobes with Ecad, RFP, GFP and Cyp2e1 antibodies depicted that tdTomato⁺ hepatocytes stayed around the central veins in the entire lobule, including the new portions after regeneration (Figure 23). Furthermore, there was a lack of detection of GFP⁺RFP⁻ hepatocytes which indicates that the newly regenerated pericentral Lgr5-GFP⁺ cells were derived exclusively from other preexisting Lgr5⁺ hepatocytes in the original lobes. No tdTomato⁺ cells were found in Sox9⁺ and Ecad⁺ cells, which suggests that Lgr5⁺ cells did not give rise to periportal hepatocytes or cholangiocytes during regeneration of the liver after PHx. (Figure 23).

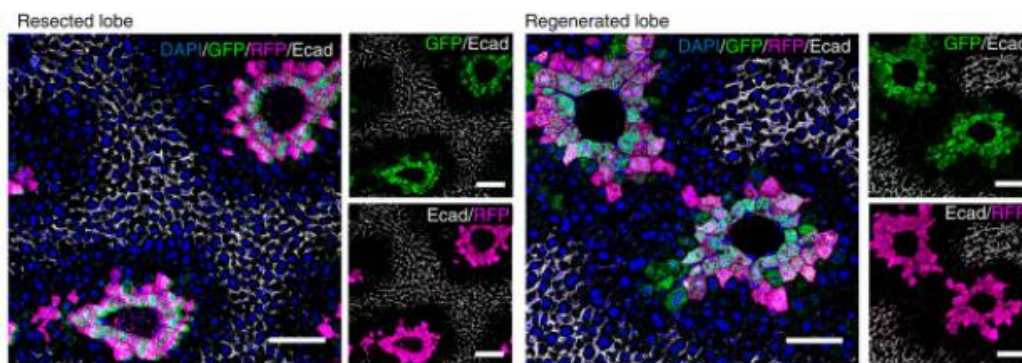


Figure 23. confocal images showing a similar immunofluorescence pattern of Lgr5-GFP⁺tdTomato⁺ population in the resected lobe compared to the regenerated lobe. Lgr5-GFP⁺tdTomato⁺ population remained

surrounding the central veins after PHx. $N=5$. (Edited from [83]).

Figure 24 depicts the similarity in the ratios between GFP+ and RFP+ in resected and re-generated lobes. This suggests that there is not a significant expansion of Lgr5 hepatocytes to others after PHx.

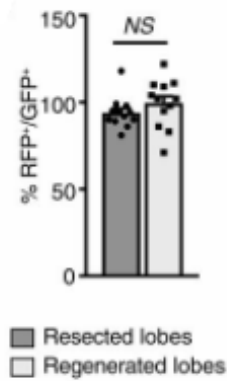


Figure 24. Quantification of the percentage of RFP+ in relation to GFP+ hepatocytes on regenerated and resected lobes. 200 cells per site were counted. (Image edited from [83]).

4.1.2.2 Lgr5+ hepatocytes are susceptible to neoplastic transformation

Figure 25 depicts the confocal images taken after the induction of DEN and doxycycline (DOX). These images show the distribution of Lgr5-GFP+tdTomato+ around the central veins at P15 without DEN injection, and at P15 and P21 (corresponding to 3 and 9 days after DEN injection).

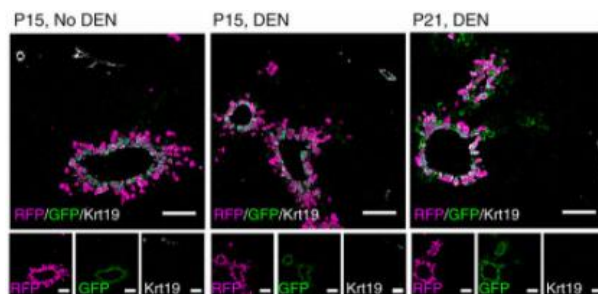


Figure 25. Experimental strategy for DEN and DOX induction for Lgr5-rtTA/TetO-Cre/R26-tdTomato mice. Distribution of Lgr5-GFP+tdTomato+ around the central veins at P15 without DEN injection, and at P15 and P21 (corresponding to 3 and 9 days after DEN injection). (Edited from [83]).

Livers harvested 8 months after DEN injection showed multiple tumors. While Lgr5+ cells only contributed to about 2% of total hepatocytes, approximately 40% of DEN-induced

tumors comprised tdTomato⁺ cells. This indicated that these tumors derived from Lgr5⁺ hepatocyte subsets. (Figure 26)

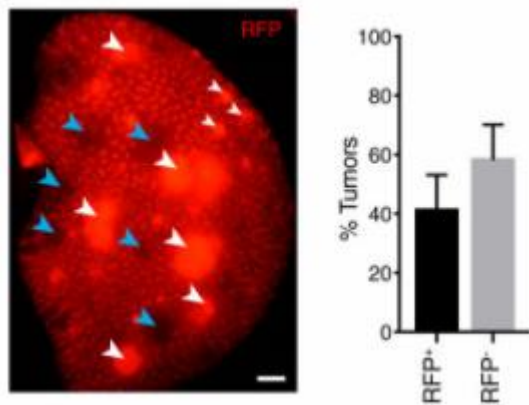


Figure 26. Fluorescent view of a tumorous liver lobe of Lgr5-rtTA/TetO-Cre/R26-tdTomato mouse 8 months after DEN induction. tdTomato⁺ are depicted in white and tdTomato⁻ are depicted in blue. Approximately a 40% of the tumors detected showed RFP⁺ (native tdTomato⁺) fluorescence. (Edited from [83]).

4.2 Actual project results

4.2.1 Hepatocyte proliferation does not follow a specific pattern

With the locating proliferative hepatocytes experiment we saw there were low numbers of proliferative hepatocytes (as expected) but we also wanted to know whether these hepatocytes were proliferating randomly or if they were following a pattern. The number of positive Ki67 cells, in pink (Figure 27), was counted for each image and tissue sample. This was done by counting how many cells away from the central vein each of the Ki67 positive cells were. The data from samples 1-4 was collected in Figure 28.

It turned out that these proliferating hepatocytes tend to just proliferate at random locations, there was not a clear pattern. Leading to the early conclusion that there is not one specific zone where proliferation takes place. However, it remains possible that some hepatocytes are still more proliferative than others.

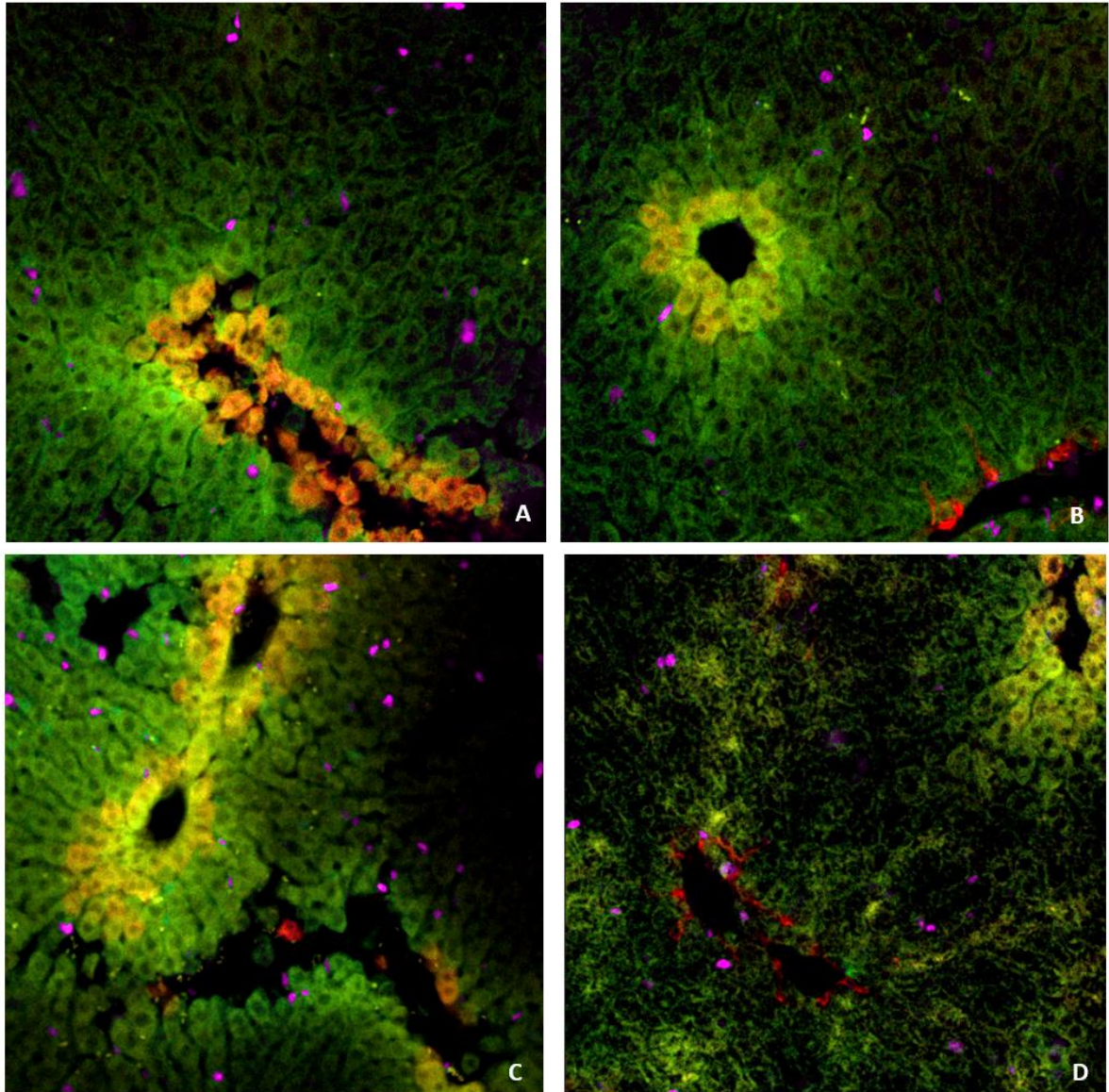


Figure 27. Location of Ki67 positive hepatocytes (in pink) with respect to the central vein (in red). (A) Image corresponding to sample 1, (B) image corresponding to sample 2, (C) image corresponding to sample 3 and (D) image corresponding to sample 4. All images were taken in a 20x magnification and using the Zeiss 710 confocal microscope.

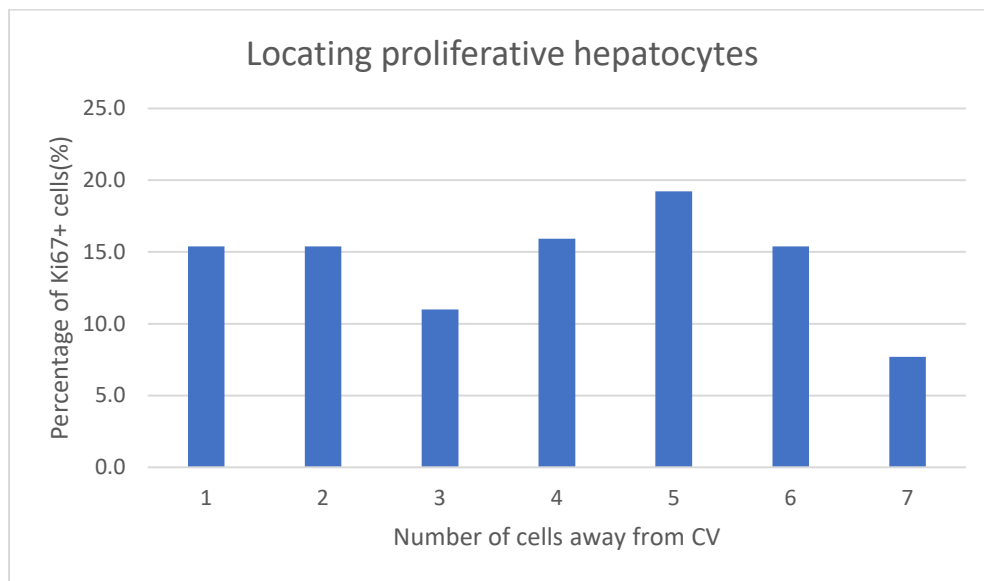


Figure 28. Graph showing the number of cells away from the central vein where the Ki67 positive hepatocytes were located.

4.2.2 Fate of proliferative hepatocytes

As described in section 4.3, to test whether some hepatocytes tend to proliferate more than others, a male and a female Ki67CreER;tdTomato mice were pulsed 2mg tamoxifen injections every other day for one month. This should have labelled the hepatocytes that proliferated during that month. After one month, the mice were kept alive for 2 more weeks with no tamoxifen injections just to let all the tamoxifen wash out from the system to prevent the labelling of new proliferative cells.

Figure 29 shows tdTomato positive cells in yellow and Ki67 positive hepatocytes in pink. Figure 30 depicts the tdTomato positive cells in green, glutamine synthetase in red and Ki67 positive cells in pink. As shown in both figures, there were few Ki67 positive cells but all the Ki67 positive cells were also positive for tdTomato. To study the distribution of these double-positive cells, the distance from the central vein was measured by counting how many cells away from the central vein (in red) these double-positives were. As depicted in Figure 31, these double-positives were located no more than 4 cells away from a central vein which suggests that these double-positive hepatocytes are spatially restricted.

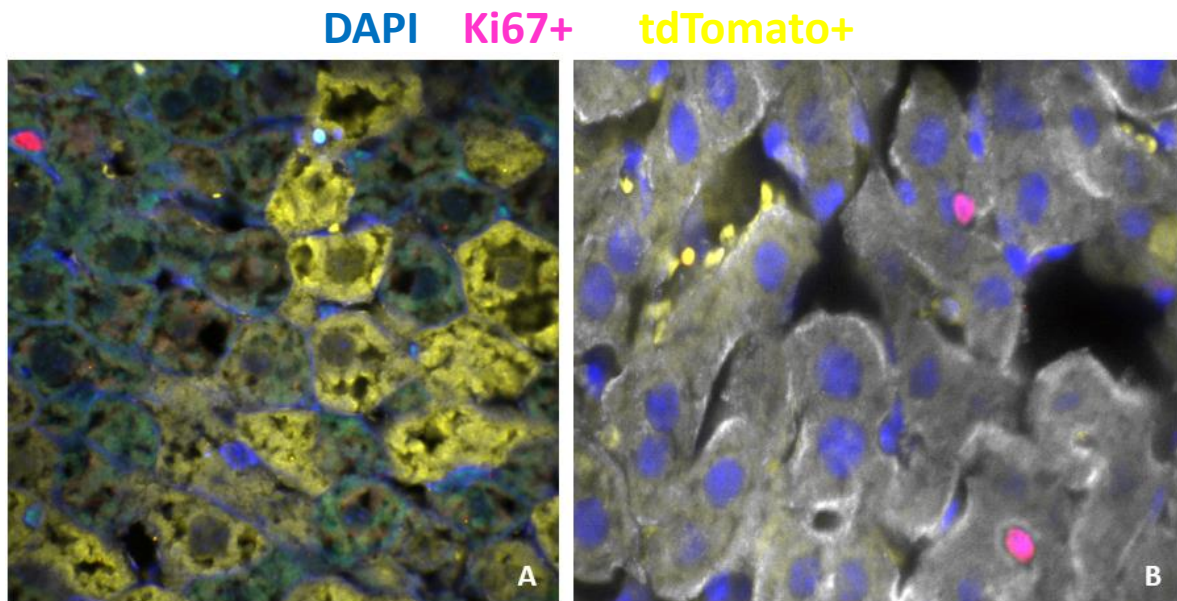


Figure 29. Figure showing *Ki67* positive and *tdTomato* positive hepatocytes. (A) image corresponding to sample 1, (B) image corresponding to sample 2. All images were taken in a 40x magnification using an RPI microscope.

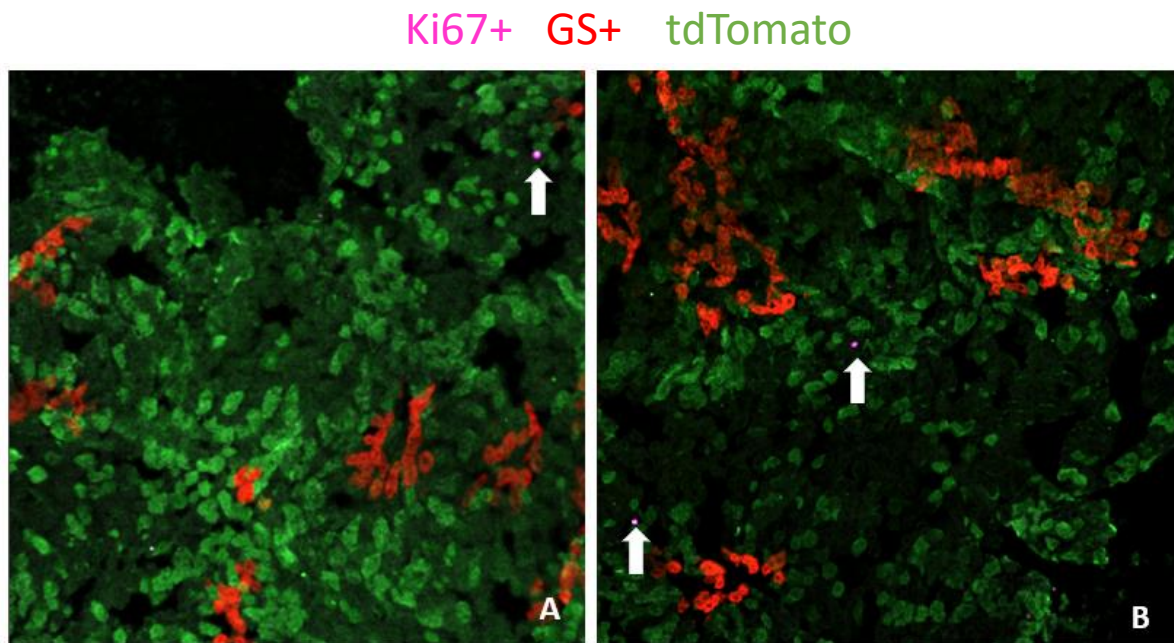


Figure 30. Figure showing *Ki67* positive (in pink) and *tdTomato* positive hepatocytes (in green) in respect to the central vein (in red). (A) image corresponding to sample 1, (B) image corresponding to sample 2. All images were taken in a 10x magnification using the Zeiss 710 confocal microscope.

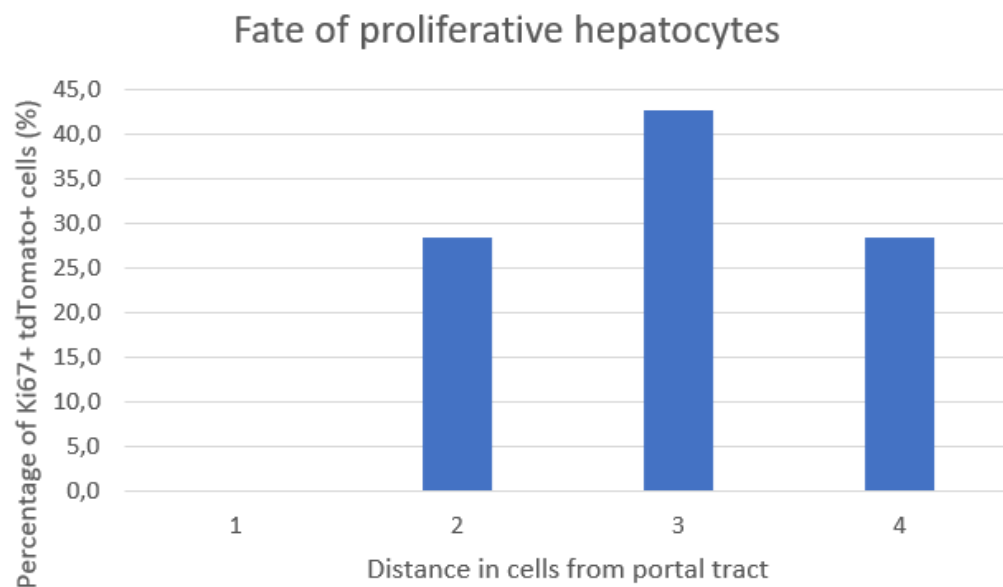


Figure 31. Graph showing the number of cells away from the central vein where the double-positive hepatocytes (Ki67 positive and tdTomato positive cells) were located.

5 Discussion

The liver, unlike any other internal organ, can completely regenerate itself after injury. This regeneration is not driven by a stem cell population but by the proliferation of differentiated hepatocytes. Although this regenerative capacity has been known for more than a few years, it is not yet clearly understood how hepatocytes in homeostasis are able to regenerate the liver after a severe injury. Some studies suggest that select hepatocytes distributed throughout the liver lobule have heightened proliferative capacity, others indicate that hepatocytes located in the pericentral zone are the source of all new hepatocytes and yet others suggest that all hepatocytes have equivalent proliferative capacity [96][82].

Clarifying the mechanism and source of hepatocyte turnover in injury and homeostasis is a crucial first step towards a better understanding of liver regeneration and the ability of hepatocytes to retain proliferative capacity unlike other differentiated cell types. With this project then, we will be able to find out more about these properties making hepatocytes so special in order to see if they can be transmitted to different cell types with the main objective of conferring regeneration properties to other vital organs.

Even though hepatocytes in different zones around the liver lobule have morphological similarities, they have heterogeneous regenerative capacity and metabolic functions. It was proposed that hepatocytes were maintained by a liver model where new hepatocytes are generated constantly at the portal vein domain and move away from the portal vein to replace the hepatocytes all over the liver lobule [97].

In 2015, Wang et al. presented a view of hepatocyte homeostasis in uninjured livers. They found a Wnt-responsive cell population residing in a held niche around the central vein. According to their study, these cells can self-renew, and they contribute to the maintenance of hepatocytes by replacing and differentiating into other hepatocytes. The presence of this pericentral hepatocyte population suggests that the mechanisms that regulate liver renewal are like other organs in which homeostatic renewal involves small stem cells populations that maintain the tissue. However, they also showed that hepatocytes are not made up of just one cell type and that they are inequivalent in replicative ability during homeostasis [28]. They proved that pericentral hepatocytes are unique and proliferate at a higher rate, an observation that was already made by Magami, Y. et al. in 2002 [93]. They concluded that pericentral cells present a diploid genome, unlike most hepatocytes, which are polyploid. By maintaining this diploid nature pericentral cells retain unlimited replicative potential just like stem cells. Finally, they stated that it is diploid Axin2⁺ cells the ones that fuel homeostatic liver renewal.

However, in 2020, Sun et al. proved that there is an equitable reparative and homeostatic potential of all hepatocytes, regardless of their ploidy status or lobular location. They stated that hepatocytes located throughout the liver can upregulate both LGR5 and Axin2 after

injury and contribute to liver regrowth on demand and not by a pericentral stem cell population. Sun et al. stated that Axin2⁺ pericentral hepatocytes have limited contribution to liver regeneration and homeostasis [82].

In 2018, Lin et al. reported that Tert⁺ hepatocytes distributed randomly in the liver lobule are responsible for the replenishment of hepatocytes during injury and liver homeostasis [98]. In 2019, Chow et al. stated that Lgr5⁺ expression in the liver was restricted to a unique hepatocyte subset adjacent to central veins. By genetic lineage tracing, they were able to see that Lgr5⁺ pericentral hepatocytes contribute, mainly, to their own lineage preservation during postnatal liver homeostasis and development. These hepatocytes also sustain their own lineage regeneration during the rapid and massive regeneration process after a two-thirds PHx. Additionally, Lgr5⁺ hepatocytes were found to be the principal cellular genesis of diethylnitrosamine (DEN)-induced hepatocellular carcinoma (HCC). These findings established an unexpected self-maintaining model for a specific subset of hepatocytes during regeneration and homeostasis of the liver and identified Lgr5⁺ pericentral hepatocytes as the major cells of genesis in HCC development [99] [83]. A future experiment will be to perform lineage tracing to determine whether there are Tert⁺ cells within the Lgr5⁺ population.

With this project, we determined that there is not a specific location for the proliferation of hepatocytes but that they appear to proliferate at random locations. This leads to the early conclusion that there is not one specific zone where proliferation takes place. This follows the conclusion shown in other studies where it is unlikely that there is one specific zone where proliferation occurs. However, it remains possible that some hepatocytes are still more proliferative than others, but they are distributed across the concentric zones of the liver.

With the fate of proliferative hepatocytes experiment, Ki67CreER;tdTomato mice were pulsed 2mg tamoxifen injections every other day for one month. This should have labelled the hepatocytes that proliferated during that month. After one month, the mice were kept alive for two more weeks with no tamoxifen injections just to let all tamoxifen wash out from the system to prevent the labelling of new proliferative hepatocytes. If it is true that there are some hepatocytes that are more likely to proliferate, then the cells that are actively proliferating at the time of harvest, Ki67⁺ cells, should be more likely to have proliferated, tdTomato⁺, in the month of labelling. It was shown that this double positive hepatocytes (Ki67+tdTomato⁺) were located no more than 4 cells away from the central vein which suggests that these double-positive hepatocytes are spatially restricted to the central vein zone as also mentioned in other studies [83] [28].

Further experiments will consist on identifying the molecular mechanism that enables their proliferative capacity. For this, we will pulse Ki67CreER;tdTomato mice with a dose of tamoxifen in order to label all proliferating hepatocytes in a day of tamoxifen pulse. After one week of the pulse, hepatocytes will be isolated using FACS to purify the tdTomato⁺ and

therefore proliferative hepatocytes. After this is done, RNA sequencing will be performed to compare the transcriptome of proliferative hepatocytes to other hepatocytes in the liver. This analysis will then provide the foundations for further insight into the unique proliferative ability of hepatocytes.

Bibliography

- [1] C. Blanpain and E. Fuchs, "Plasticity of epithelial stem cells in tissue regeneration," *Science* (80-.), vol. 344, no. 6189, pp. 1242281–1242281, Jun. 2014.
- [2] G. K. Michalopoulos, "Liver regeneration," *J. Cell. Physiol.*, vol. 213, no. 2, pp. 286–300, Nov. 2007.
- [3] "The Liver: Introduction and Index." [Online]. Available: <http://www.vivo.colostate.edu/hbooks/pathophys/digestion/liver/index.html>. [Accessed: 11-Aug-2020].
- [4] "Anatomy and physiology of the liver." [Online]. Available: <https://www.rnceus.com/ld/ldanat.html>. [Accessed: 11-Aug-2020].
- [5] "How the Liver Works." [Online]. Available: <https://www.stanfordchildrens.org/en/topic/default?id=how-the-liver-works-90-P02006>. [Accessed: 11-Aug-2020].
- [6] "Printed from STUDENT CONSULT: Berne and Levy Physiology 6E - The Online Medical Library for Students plus USMLE Steps 123 (ver. 2.9)." [Online]. Available: <http://users.atw.hu/blp6/BLP6/HTML/C0319780323045827.htm>. [Accessed: 12-Aug-2020].
- [7] "Overview - Hepatic Circulation - NCBI Bookshelf." [Online]. Available: <https://www.ncbi.nlm.nih.gov/books/NBK53069/>. [Accessed: 12-Aug-2020].
- [8] A. Damania, E. Jain, and A. Kumar, "Advancements in in vitro hepatic models: Application for drug screening and therapeutics," *Hepatol. Int.*, vol. 8, no. 1, pp. 23–38, 2014.
- [9] H. Tsutsui and S. Nishiguchi, "Importance of kupffer cells in the development of acute liver injuries in mice," *International Journal of Molecular Sciences*, vol. 15, no. 5. Molecular Diversity Preservation International, pp. 7711–7730, 05-May-2014.
- [10] L. D. Deleve, "Liver sinusoidal endothelial cells in hepatic fibrosis," *Hepatology*, vol. 61, no. 5, pp. 1740–1746, May 2015.
- [11] W. M. Haschek, C. G. Rousseaux, and M. A. Wallig, "The Liver," in *Fundamentals of Toxicologic Pathology*, Elsevier, 2010, pp. 197–235.
- [12] K. Iguchi and N. Koyanagi, "Hepatic circulation," *Respir. Circ.*, vol. 30, no. 7, pp. 732–734, Jul. 1982.
- [13] "MacSween's Pathology of the Liver - 7th Edition." [Online]. Available: <https://www.elsevier.com/books/macsweens-pathology-of-the-liver/burt/978-0-7020-6697-9>. [Accessed: 12-Aug-2020].
- [14] L. M. Reid, A. S. Fiorino, S. H. Sigal, S. Brill, and P. A. Holst, "Extracellular matrix gradients in the space of disse: Relevance to liver biology," *Hepatology*, vol. 15, no. 6. Hepatology, pp. 1198–1203, 1992.
- [15] T. Kalogeris, C. P. Baines, M. Krenz, and R. J. Korthuis, "Cell Biology of Ischemia/Reperfusion Injury," in *International Review of Cell and Molecular Biology*, vol. 298, Elsevier Inc., 2012, pp. 229–317.
- [16] S. L. Friedman, "Hepatic stellate cells: Protean, multifunctional, and enigmatic cells of the liver," *Physiological Reviews*, vol. 88, no. 1. NIH Public Access, pp. 125–172, Jan-2008.
- [17] H. Senoo, K. Yoshikawa, M. Morii, M. Miura, K. Imai, and Y. Mezaki, "Hepatic stellate cell (vitamin A-storing cell) and its relative – past, present and future," *Cell Biol. Int.*, vol. 34, no. 12, pp. 1247–1272, Dec. 2010.
- [18] C. Yin, K. J. Evason, K. Asahina, and D. Y. R. Stainier, "Hepatic stellate cells in liver development, regeneration, and cancer," *Journal of Clinical Investigation*, vol. 123, no. 5. J Clin Invest, pp. 1902–1910, 01-May-2013.
- [19] J. M. Crawford, "1. THE INTRAHEPATIC BILIARY TREE," *Principles of Medical Biology*, vol. 15, no. C. Elsevier, pp. 1–20, 01-Jan-2004.

- [20] T. A. Roskams *et al.*, "Nomenclature of the finer branches of the biliary tree: Canals, ductules, and ductular reactions in human livers," *Hepatology*, vol. 39, no. 6. pp. 1739–1745, Jun-2004.
- [21] "SIU SOM Histology GI." [Online]. Available: <http://www.siumed.edu/~dking2/erg/GI162b.htm>. [Accessed: 12-Aug-2020].
- [22] "Liver Structure | BioNinja." [Online]. Available: <https://ib.bioninja.com.au/options/option-d-human-physiology/d3-functions-of-the-liver/liver-structure.html>. [Accessed: 12-Aug-2020].
- [23] A. L. Mescher, *Junqueira's Basic Histology text and atlas*. McGraw-Hill Education, 2013.
- [24] A. B. Rogers and R. Z. Dintzis, "Liver and Gallbladder," in *Comparative Anatomy and Histology*, Elsevier Inc., 2012, pp. 193–201.
- [25] "What are Hepatocytes? (with pictures)." [Online]. Available: <https://www.wisegeek.com/what-are-hepatocytes.htm#>. [Accessed: 13-Aug-2020].
- [26] "Cell types. Hepatocyte. Atlas of Plant and Animal Histology." [Online]. Available: <https://mmegias.webs.uvigo.es/02-english/8-tipos-celulares/hepatocito.php>. [Accessed: 13-Aug-2020].
- [27] "Ground glass hepatocyte - Libre Pathology." [Online]. Available: https://librepathology.org/wiki/Ground_glass_hepatocyte. [Accessed: 13-Aug-2020].
- [28] B. Wang, L. Zhao, M. Fish, C. Y. Logan, and R. Nusse, "Self-renewing diploid Axin2 + cells fuel homeostatic renewal of the liver," *Nature*, vol. 524, no. 7564, pp. 180–185, Aug. 2015.
- [29] K. B. Halpern *et al.*, "Single-cell spatial reconstruction reveals global division of labour in the mammalian liver," *Nature*, vol. 542, no. 7641, pp. 1–5, Feb. 2017.
- [30] P. Gissen and I. M. Arias, "Structural and functional hepatocyte polarity and liver disease," *Journal of Hepatology*, vol. 63, no. 4. Elsevier, pp. 1023–1037, 01-Oct-2015.
- [31] "Use of cultured cells to study alcohol metabolism - PubMed." [Online]. Available: <https://pubmed.ncbi.nlm.nih.gov/17718409/>. [Accessed: 13-Aug-2020].
- [32] A. Müsch, "The special case of hepatocytes: unique tissue architecture calls for a distinct mode of cell division," *Bioarchitecture*, vol. 4, no. 2, pp. 47–52, 2014.
- [33] S. Paxton, M. Peckham, A. Knibbs, S. Paxton, A. Knibbs, and M. Peckham, "The Leeds Histology Guide." 2003.
- [34] "Digestive: The Histology Guide." [Online]. Available: http://www.histology.leeds.ac.uk/digestive/liver_hepatocyte.php. [Accessed: 13-Aug-2020].
- [35] A. Kalra and F. Tuma, *Physiology, Liver*. StatPearls Publishing, 2018.
- [36] "Liver – Anatomy and Function of the Human Liver." [Online]. Available: https://www.innerbody.com/image_digeov/card10-new2.html. [Accessed: 13-Aug-2020].
- [37] "Hepatocyte - an overview | ScienceDirect Topics." [Online]. Available: <https://www.sciencedirect.com/topics/medicine-and-dentistry/hepatocyte>. [Accessed: 13-Aug-2020].
- [38] N. Barker, "Adult intestinal stem cells: Critical drivers of epithelial homeostasis and regeneration," *Nature Reviews Molecular Cell Biology*, vol. 15, no. 1. Nature Publishing Group, pp. 19–33, 11-Jan-2014.
- [39] M. R. Lemus *et al.*, "El hepatocito como un ejemplo de la interacción entre la biología celular y las rutas metabólicas," 2017.
- [40] Y. Malato *et al.*, "Fate tracing of mature hepatocytes in mouse liver homeostasis and regeneration," *J. Clin. Invest.*, vol. 121, no. 12, pp. 4850–4860, Dec. 2011.
- [41] D. W. Crabb, "Pathogenesis of alcoholic liver disease: Newer mechanisms of injury," *Keio J. Med.*, vol. 48, no. 4, pp. 184–188, 1999.
- [42] I. Bergheim, C. J. McClain, and G. E. Arteel, "Treatment of alcoholic liver disease,"

- Dig. Dis.*, vol. 23, no. 3–4, pp. 275–284, Feb. 2006.
- [43] V. L. Massey and G. E. Arteel, “Acute alcohol-induced liver injury,” *Frontiers in Physiology*, vol. 3 JUN. Frontiers Media SA, 2012.
 - [44] S. Q. Yang, H. Z. Lin, M. D. Lane, M. Clemens, and A. M. Diehl, “Obesity increases sensitivity to endotoxin liver injury: Implications for the pathogenesis of steatohepatitis,” *Proc. Natl. Acad. Sci. U. S. A.*, vol. 94, no. 6, pp. 2557–2562, Mar. 1997.
 - [45] A. A. Nanji, U. Khettry, and S. M. H. Sadrzadeh, “Lactobacillus Feeding Reduces Endotoxemia and Severity of Experimental Alcoholic Liver (Disease),” *Proc. Soc. Exp. Biol. Med.*, vol. 205, no. 3, pp. 243–247, 1994.
 - [46] T. H. H. Y, K. S, Y. H, and I. H, “Long-term ethanol feeding enhances susceptibility of the liver to orally administered lipopolysaccharides in rats,” *Alcohol. Clin. Exp. Res.*, vol. 26, no. 8 Suppl, 2002.
 - [47] J. C. Lambert, Z. Zhou, L. Wang, Z. Song, C. J. McClain, and Y. J. Kang, “Prevention of alterations in intestinal permeability is involved in zinc inhibition of acute ethanol-induced liver damage in mice,” *J. Pharmacol. Exp. Ther.*, vol. 305, no. 3, pp. 880–886, Jun. 2003.
 - [48] C. Bunchorntavakul and K. R. Reddy, “Acetaminophen-related Hepatotoxicity,” *Clinics in Liver Disease*, vol. 17, no. 4. Clin Liver Dis, pp. 587–607, Nov-2013.
 - [49] E. Michna, M. S. Duh, C. Korves, and J. L. Dahl, “Removal of opioid/acetaminophen combination prescription pain medications: Assessing the evidence for hepatotoxicity and consequences of removal of these medications,” *Pain Medicine*, vol. 11, no. 3. Blackwell Publishing Inc., pp. 369–378, 2010.
 - [50] K. F. Murray, N. Hadzic, S. Wirth, M. Bassett, and D. Kelly, “Drug-related hepatotoxicity and acute liver failure,” *Journal of Pediatric Gastroenterology and Nutrition*, vol. 47, no. 4. Lippincott Williams and Wilkins, pp. 395–405, 2008.
 - [51] R. Clark, J. E. Fisher, I. S. Sketris, and G. M. Johnston, “Population prevalence of high dose paracetamol in dispensed paracetamol/opioid prescription combinations: An observational study,” *BMC Clin. Pharmacol.*, vol. 12, Jun. 2012.
 - [52] H. Jaeschke and M. R. McGill, “Cytochrome P450-derived versus mitochondrial oxidant stress in acetaminophen hepatotoxicity,” *Toxicology Letters*, vol. 235, no. 3. Elsevier Ireland Ltd, pp. 216–217, 05-Jun-2015.
 - [53] H. Jaeschke, M. R. McGill, and A. Ramachandran, “Oxidant stress, mitochondria, and cell death mechanisms in drug-induced liver injury: Lessons learned from acetaminophen hepatotoxicity,” *Drug Metabolism Reviews*, vol. 44, no. 1. Drug Metab Rev, pp. 88–106, Feb-2012.
 - [54] H. Jaeschke, C. D. Williams, A. Ramachandran, and M. L. Bajt, “Acetaminophen hepatotoxicity and repair: The role of sterile inflammation and innate immunity,” *Liver International*, vol. 32, no. 1. Liver Int, pp. 8–20, Jan-2012.
 - [55] M. R. McGill and H. Jaeschke, “Metabolism and disposition of acetaminophen: Recent advances in relation to hepatotoxicity and diagnosis,” *Pharmaceutical Research*, vol. 30, no. 9. Pharm Res, pp. 2174–2187, Sep-2013.
 - [56] A. Abu Rmilah, W. Zhou, E. Nelson, L. Lin, B. Amiot, and S. L. Nyberg, “Understanding the marvels behind liver regeneration,” *Wiley Interdisciplinary Reviews: Developmental Biology*, vol. 8, no. 3. John Wiley and Sons Inc., p. e340, 01-May-2019.
 - [57] S. A. Mao, J. M. Glorioso, and S. L. Nyberg, “Liver regeneration,” *Translational Research*, vol. 163, no. 4. Mosby Inc., pp. 352–362, 2014.
 - [58] G. K. Michalopoulos and M. C. DeFrances, “Liver regeneration,” *Science*, vol. 276, no. 5309. American Association for the Advancement of Science, pp. 60–65, 04-Apr-1997.
 - [59] D. Palmes and H. U. Spiegel, “Animal models of liver regeneration,” *Biomaterials*, vol. 25, no. 9, pp. 1601–1611, 2004.

- [60] T. Cantz, M. P. Manns, and M. Ott, "Stem cells in liver regeneration and therapy," *Cell and Tissue Research*, vol. 331, no. 1, pp. 271–282, Jan-2008.
- [61] T. Sokabe *et al.*, "Differential regulation of urokinase-type plasminogen activator expression by fluid shear stress in human coronary artery endothelial cells," *Am. J. Physiol. - Hear. Circ. Physiol.*, vol. 287, no. 5 56-5, Nov. 2004.
- [62] T. H. Kim, W. M. Mars, D. B. Stolz, and G. K. Michalopoulos, "Expression and activation of pro-MMP-2 and pro-MMP-9 during rat liver regeneration," *Hepatology*, vol. 31, no. 1, pp. 75–82, 2000.
- [63] P. S. Olsen, S. S. Poulsen, and P. Kirkegaard, "Adrenergic effects on secretion of epidermal growth factor from Brunner's glands," *Gut*, vol. 26, no. 9, pp. 920–927, 1985.
- [64] M. Jo, D. B. Stolz, J. E. Esplen, K. Dorko, G. K. Michalopoulos, and S. C. Strom, "Cross-talk between epidermal growth factor receptor and c-Met signal pathways in transformed cells," *J. Biol. Chem.*, vol. 275, no. 12, pp. 8806–8811, Mar. 2000.
- [65] N. Fausto, J. S. Campbell, and K. J. Riehle, "Liver regeneration," *Hepatology*, vol. 43, no. 2 SUPPL. 1. Hepatology, Feb-2006.
- [66] W. Li, X. Liang, J. I. Leu, K. Kovalovich, G. Ciliberto, and R. Taub, "Global changes in interleukin-6-dependent gene expression patterns in mouse livers after partial hepatectomy," *Hepatology*, vol. 33, no. 6, pp. 1377–1386, 2001.
- [67] S. Hata, M. Namae, and H. Nishina, "Liver development and regeneration: From laboratory study to clinical therapy," *Development Growth and Differentiation*, vol. 49, no. 2. Dev Growth Differ, pp. 163–170, Feb-2007.
- [68] A. Zimmermann, "Regulation of liver regeneration," *Nephrol. Dial. Transplant.*, vol. 19, no. SUPPL. 4, Jul. 2004.
- [69] J. O. Russell and S. P. Monga, "Wnt/ β -Catenin Signaling in Liver Development, Homeostasis, and Pathobiology," *Annual Review of Pathology: Mechanisms of Disease*, vol. 13. Annual Reviews Inc., pp. 351–378, 24-Jan-2018.
- [70] K. Bartscherer, N. Pelte, D. Ingelfinger, and M. Boutros, "Secretion of Wnt Ligands Requires Evi, a Conserved Transmembrane Protein," *Cell*, vol. 125, no. 3, pp. 523–533, May 2006.
- [71] P. Bhanot *et al.*, "A new member of the frizzled family from Drosophila functions as a wingless receptor," *Nature*, vol. 382, no. 6588, pp. 225–231, Jul. 1996.
- [72] K. M. Cadigan and R. Nusse, "Wnt signaling: A common theme in animal development," *Genes and Development*, vol. 11, no. 24. Cold Spring Harbor Laboratory Press, pp. 3286–3305, 15-Dec-1997.
- [73] C. M. Morell, R. Fiorotto, L. Fabris, and M. Strazzabosco, "Notch signalling beyond liver development: Emerging concepts in liver repair and oncogenesis," *Clinics and Research in Hepatology and Gastroenterology*, vol. 37, no. 5. Clin Res Hepatol Gastroenterol, pp. 447–454, Nov-2013.
- [74] B. Z. Stanger and L. Greenbaum, "The role of paracrine signals during liver regeneration," *Hepatology*, vol. 56, no. 4. Hepatology, pp. 1577–1579, Oct-2012.
- [75] S. S. Nijjar, H. A. Crosby, L. Wallace, S. G. Hubscher, and A. J. Strain, "Notch receptor expression in adult human liver: A possible role in bile duct formation and hepatic neovascularization," *Hepatology*, vol. 34, no. 6, pp. 1184–1192, 2001.
- [76] F. Böhm, U. A. Köhler, T. Speicher, and S. Werner, "Regulation of liver regeneration by growth factors and cytokines," *EMBO Molecular Medicine*, vol. 2, no. 8. EMBO Mol Med, pp. 294–305, Aug-2010.
- [77] L. Wang *et al.*, "Disruption of the transcription factor recombination signal-binding protein-Jk (RBP-J) leads to veno-occlusive disease and interfered liver regeneration in mice," *Hepatology*, vol. 49, no. 1, pp. 268–277, 2009.
- [78] M. Liu and P. Chen, "Proliferation-inhibiting pathways in liver regeneration (Review)," *Molecular Medicine Reports*, vol. 16, no. 1. Spandidos Publications, pp. 23–35, 01-Jul-2017.

- [79] G. K. Michalopoulos, "Liver regeneration after partial hepatectomy: Critical analysis of mechanistic dilemmas," *Am. J. Pathol.*, vol. 176, no. 1, pp. 2–13, 2010.
- [80] I. N. Hines *et al.*, "Impaired liver regeneration and increased oval cell numbers following T cell-mediated hepatitis," *Hepatology*, vol. 46, no. 1, pp. 229–241, Jul. 2007.
- [81] C. M. Samson *et al.*, "Transforming growth factor- β 1 induces hepatocyte apoptosis by a c-Jun independent mechanism," *Surgery*, vol. 132, no. 3, pp. 441–449, Sep. 2002.
- [82] T. Sun *et al.*, "AXIN2+ Pericentral Hepatocytes Have Limited Contributions to Liver Homeostasis and Regeneration," *Cell Stem Cell*, vol. 26, no. 1, p. 97–107.e6, Jan. 2020.
- [83] C. H. Ang *et al.*, "Lgr5+ pericentral hepatocytes are self-maintained in normal liver regeneration and susceptible to hepatocarcinogenesis.," *Proc. Natl. Acad. Sci. U. S. A.*, vol. 116, no. 39, pp. 19530–19540, Sep. 2019.
- [84] S. Bruno and Z. Darzynkiewicz, "Cell cycle dependent expression and stability of the nuclear protein detected by Ki-67 antibody in HL-60 cells," *Cell Prolif.*, vol. 25, no. 1, pp. 31–40, Jan. 1992.
- [85] T. Scholzen and J. Gerdes, "The Ki-67 protein: From the known and the unknown," *J. Cell. Physiol.*, vol. 182, no. 3, pp. 311–322, Mar. 2000.
- [86] S. Cuylen *et al.*, "Ki-67 acts as a biological surfactant to disperse mitotic chromosomes," *Nature*, vol. 535, no. 7611, pp. 308–312, Jul. 2016.
- [87] "Glutamine Synthetase (GS-6)," no. zone 3, p. 8900, 2014.
- [88] J. Shen, R. T. Bronson, D. F. Chen, W. Xia, D. J. Selkoe, and S. Tonegawa, "Skeletal and CNS defects in Presenilin-1-deficient mice.," *Cell*, vol. 89, no. 4, pp. 629–39, May 1997.
- [89] Y. Li, R. S. Erzurumlu, C. Chen, S. Jhaveri, and S. Tonegawa, "Whisker-related neuronal patterns fail to develop in the trigeminal brainstem nuclei of NMDAR1 knockout mice.," *Cell*, vol. 76, no. 3, pp. 427–37, Feb. 1994.
- [90] S. A. Murray, J. T. Eppig, D. Smedley, E. M. Simpson, and N. Rosenthal, "Beyond knockouts: cre resources for conditional mutagenesis," *Mamm. Genome*, vol. 23, no. 9–10, pp. 587–599, Oct. 2012.
- [91] J. E. Sulston, E. Schierenberg, J. G. White, and J. N. Thomson, "The embryonic cell lineage of the nematode *Caenorhabditis elegans*," *Dev. Biol.*, vol. 100, no. 1, pp. 64–119, Nov. 1983.
- [92] S. H. Sigal *et al.*, "Partial hepatectomy-induced polyploidy attenuates hepatocyte replication and activates cell aging events," *Am. J. Physiol. - Gastrointest. Liver Physiol.*, vol. 276, no. 5 39-5, 1999.
- [93] J. E. Guidotti, O. Br  gerie, A. Robert, P. Debey, C. Brechot, and C. Desdouets, "Liver cell polyploidization: A pivotal role for binuclear hepatocytes," *J. Biol. Chem.*, vol. 278, no. 21, pp. 19095–19101, May 2003.
- [94] B. Ohlstein and A. Spradling, "The adult *Drosophila* posterior midgut is maintained by pluripotent stem cells," *Nature*, vol. 439, no. 7075, pp. 470–474, Jan. 2006.
- [95] L. Comai, "The advantages and disadvantages of being polyploid," *Nature Reviews Genetics*, vol. 6, no. 11. Nat Rev Genet, pp. 836–846, Nov-2005.
- [96] B. Wang, L. Zhao, M. Fish, C. Y. Logan, and R. Nusse, "Self-renewing diploid Axin2 + cells fuel homeostatic renewal of the liver," *Nature*, vol. 524, no. 7564, pp. 180–185, 2015.
- [97] G. ZAJICEK, R. OREN, and M. WEINREB, "The streaming liver," *Liver*, vol. 5, no. 6, pp. 293–300, 1985.
- [98] S. Lin *et al.*, "Distributed hepatocytes expressing telomerase repopulate the liver in homeostasis and injury," *Nature*, vol. 556, no. 7700, pp. 244–248, 2018.
- [99] C. H. Ang *et al.*, "Lgr5+ pericentral hepatocytes are self-maintained in normal liver regeneration and susceptible to hepatocarcinogenesis," *Proc. Natl. Acad. Sci. U. S.*

A., vol. 116, no. 39, pp. 19530–19540, Sep. 2019.

List of Figures

| | |
|--|----|
| Figure 1. Anatomy of the liver [5]. | 6 |
| Figure 2. Blood flow showing the supplied blood to the liver from the hepatic artery and portal vein. | 7 |
| Figure 3. Architecture of the liver and biliary tract. Blood flows through the liver sinusoids emptying into the central vein of each lobule. (Image created with Biorender application)..... | 8 |
| Figure 4. Structure of the liver. Hepatic sinusoids are formed by Kupffer cells and sinusoidal endothelial cells. Hepatocytes are localized in the space of Disse, outside of the sinusoid. (Image created using Biorender application). | 9 |
| Figure 5. Histological view of the portal triad. Hepatic artery, Bile duct and portal vein [21]...... | 10 |
| Figure 6. Structure of the functional units, lobules, of the liver. Adapted from [23]. ... | 11 |
| Figure 7. Arrangement of hepatocytes in sheets of one cell in thickness. [27] | 12 |
| Figure 8. Ultrastructure of hepatocyte cells. [23] | 13 |
| Figure 9. Partial hepatectomy in a mice liver [57]. | 17 |
| Figure 10. Temporal sequence of events after a partial hepatectomy [56]. | 19 |
| Figure 11. simplified overview of the experiment that will be conducted. | 24 |
| Figure 12. Simplified overview of the experiment that will be conducted. | 25 |
| Figure 13. Staining of pericentral hepatocytes revealing the central veins [87]. | 26 |
| Figure 14. Staining of bile ducts revealing the location of the portal tracts. | 27 |
| Figure 15. setup of the perfusion system used during the experiment. | 30 |
| Figure 16. Surgical procedure performed to perfuse and harvest liver tissue. | 31 |
| Figure 17. Display of the tissue samples in a 24 well plate. | 33 |
| Figure 18. display of the cryosectioned liver tissue from both liver samples. Sample 1 corresponds to the liver tissue from the male Ki67CreER;tdTomato mouse and sample 2 corresponds to the female Ki67CreER;tdTomato mouse. | 34 |
| Figure 19. Axin 2+ cells self-renew. A) Pericentral hepatocytes labelled in Axin2-CreERT2;Rosa26-mTmGflox mice after the administration of five consecutive doses of tamoxifen. Traced for 7 days. B) After 90 days of tracing. And C) after 365 days of tracing, show that all pericentral hepatocytes remained labelled. (Figure edited from [28])..... | 35 |
| Figure 20. Axin2+ cells proliferate faster than other hepatocytes. The image shows the quantification of EdU+ cells within Axin+ and Axin- hepatocyte populations. N=5 mice. (Figure edited from [28])..... | 36 |
| Figure 21. Axin2+ cells are mostly diploid. A) FACS plot of all hepatocytes stained with Hoechst 33342. Gated for 2N (diploid), 4N (tetraploid) and 8N+ (octaploid or more) cells. B) FACS plot of Axin2+ cells stained with Hoechst 33342. Gated the same way as in A. C) Ploid distribution: unsorted hepatocyte population on the left, Axin2+ hepatocyte population on the middle and labelled hepatocytes after lineage tracing for 1 year on the right. N=3 mice per group. (Figure edited from [28]) | 36 |
| Figure 22. experimental strategy for PHx experiments performed on Lgr5-rtTA/TetO-Cre/R26-tdTomato mice. Images represent the right liver lobe adult control and Lgr5-rtTA/TetO-Cre/R26-tdTomato mice harvested 14 days after PHx. N=5 mice. (Figure edited from [83]). | 37 |
| Figure 23. confocal images showing a similar immunofluorescence pattern of Lgr5-GFP+tdTomato+ population in the resected lobe compared to the regenerated lobe. Lgr5-GFP+tdTomato+ population remained surrounding the central veins after PHx. N=5. (Edited from [83]). | 37 |
| Figure 24. Quantification of the percentage of RFP+ in relation to GFP+ hepatocytes on regenerated and resected lobes. 200 cells per site were counted. (Image edited from [83]). | 38 |

| | |
|---|----|
| Figure 25. Experimental strategy for DEN and DOX induction for Lgr5-rtTA/TetO-Cre/R26-tdTomato mice. Distribution of Lgr5-GFP+tdTomato+ around the central veins at P15 without DEN injection, and at P15 and P21 (corresponding to 3 and 9 days after DEN injection). (Edited from [83]). | 38 |
| Figure 26. Fluorescent view of a tumorous liver lobe of Lgr5-rtTA/TetO-Cre/R26-tdTomato mouse 8 months after DEN induction. tdTomato+ are depicted in white and tdTomato- are depicted in blue. Approximately a 40% of the tumors detected showed RFP+ (native tdTomato+) fluorescence. (Edited from [83]). | 39 |
| Figure 27. Location of Ki67 positive hepatocytes (in pink) with respect to the central vein (in red). (A) Image corresponding to sample 1, (B) image corresponding to sample 2, (C) image corresponding to sample 3 and (D) image corresponding to sample 4. All images were taken in a 20x magnification and using the Zeiss 710 confocal microscope. | 40 |
| Figure 28. Graph showing the number of cells away from the central vein where the Ki67 positive hepatocytes were located. | 41 |
| Figure 29. Figure showing Ki67 positive and tdTomato positive hepatocytes. (A) image corresponding to sample 1, (B) image corresponding to sample 2. All images were taken in a 40x magnification using an RPI microscope. | 42 |
| Figure 30. Figure showing Ki67 positive (in pink) and tdTomato positive hepatocytes (in green) in respect to the central vein (in red). (A) image corresponding to sample 1, (B) image corresponding to sample 2. All images were taken in a 10x magnification using the Zeiss 710 confocal microscope. | 42 |
| Figure 31. Graph showing the number of cells away from the central vein where the double-positive hepatocytes (Ki67 positive and tdTomato positive cells) were located. | 43 |

List of Tables

| | |
|--|----|
| Table 1. Summary of the different characteristics of the mice used for this experiment..... | 31 |
| Table 2. Primary and secondary antibodies used to immunostain tissue samples. .. | 33 |
| Table 3. List of primary and secondary antibodies used to immunostain samples ED1.1 and ED2.1..... | 34 |
| Table 4. list of primary and secondary antibodies used to immunostain samples ED1.2 and ED2.2..... | 34 |

List of Abbreviations

| | |
|------------------|-----------------------------------|
| ADL | Alcoholic Liver Disease |
| APAP | Acetaminophen |
| ATP | Adenosine triphosphate |
| B-CDC | Beta cantenin degradation complex |
| CCl ₄ | Carbon tetrachloride |
| CK1 | Casein kinase 1 |
| CK-19 | Cytokeratin 19 |
| CYP2E1 | Cytochrome P450 2E1 |
| DEN | Diethylnitrosamine |
| DILI | Drug-induced liver injury |
| ECM | Extracellular matrix |
| EdU | 5-ethynyl-2'-deoxyuridine |
| EGF | Epidermal growth factor |
| EGFR | Epidermal growth factor receptor |
| FDP | Fibrinogen degradation product |
| GS | Glutamine Synthetase |
| GSH | Glutathione |
| HCC | Hepatocellular carcinoma |
| HGF | Hepatic growth factor |
| HGFR | Hepatic growth factor receptor |
| HPC | Hepatic progenitor cells |
| IKB | Inhibitory KB |
| IKK | Inhibitory KB kinase |
| IL6 | Interleukin 6 |
| JNK | c-Jun N-terminal kinase |
| KCs | Kupffer Cells |
| LPS | Lipopolysaccharides |
| LPS | Lipopoly-saccharide |
| LSECs | Liver Sinusoidal Endothelial Cell |
| MMP | Matrix metalloproteinases |
| NAPQI | N-acetyl-para-benzo-quinone imine |
| NF-KB | Nuclear factor KB |
| NPCs | Non-parenchymal Cells |
| OCT | Optimal cutting temperature |
| PHx | Partial Hepatectomy |
| SAPK | Stress-activated protein kinase |
| SER | Smooth Endoplasmic Reticulum |
| TF | Transcription factor |
| TNF | Tumor necrosis factor |
| TNF α | Tumor necrosis factor alpha |
| uPA | Urokinase plasminogen activator |
| WIs | Wntless |

A: Preparation of the reagents used in this study

A.1 Immunostaining and clearing tissue slices

N-methylacetamide is toxic and should be handled in a fume hood with waste collected for proper disposal

- Sodium citrate antigen retrieval buffer
 - For 1 L
 - 2.94 g Tri-sodium citrate dihydrate (10 mM)
 - 500 μ L Tween 20 (0.05%)
 - 1000 mL Water
 - pH to 6.0 with 1 M HCl
 - Store at room temperature for up to 3 months, store at 4°C indefinitely
- Tx buffer
 - Prepare fresh
 - For 40 mL
 - 80 mg Gelatin (0.2%)
 - 2.5 mL 5M NaCl (300 mM)
 - 120 μ L Triton X-100 (0.3%)
 - 37.5 mL PBS
 - Incubate at 42°C for 30 minutes to dissolve gelatin and store at 4°C indefinitely between steps
- 40% N-methylacetamide
 - Melt N-methylacetamide in 37°C water bath prior to dilution
 - For 100 mL
 - 40 mL N-methylacetamide
 - 60 mL PBS
 - Store at room temperature
- Ce3D clearing solution
 - For 40 mL
 - 16 mL 40% N-methylacetamide
 - 32 g Histodenz
 - 6 mL 40% N-methylacetamide
 - 40 μ L Triton X-100 (0.1%)
 - 200 μ L 1-thioglycerol (0.5%)
 - Add reagents in order and mix at 37°C with shaking to facilitate dissolution
 - Will require at least 1 hour to dissolve
 - Can store excess at room temperature for up to several months

A.2 Immunostaining

Reagents

Extraction buffer

- Prepare fresh
- For 1 mL
 - 10 μ L Triton X-100 (1%)
 - 990 μ L PBS

Blocking buffer

- Prepare fresh
- For 25 mL
 - 750 mg Bovine serum albumin (BSA) fraction V (3%)
 - 75 μ L Triton X-100 (0.3%)
 - 25 mL PBS

1. Cryosection
2. Leave slices at room temperature overnight
3. Rinse slides in PBS for 5 minutes
4. Antigen retrieval
5. Remove coplin jar from pressure cooker, allow slide to cool in coplin jar, and rinse slide in PBS for 5 minutes
6. Outline sections in hydrophobic pen
7. Incubate sections with extraction buffer at room temperature for 15 minutes
8. Incubate sections with blocking buffer at room temperature for 1 hour
9. Incubate sections with primary antibodies at room temperature overnight
10. Wash sections with blocking buffer at room temperature for 5-10 minutes 3x
11. Incubate sections with secondary antibodies at room temperature for 1-2 hours
12. Wash sections with blocking buffer at room temperature for 5-10 minutes 2x
13. Wash sections with PBS at room temperature for 5-10 minutes
14. Mount slides with antifade reagent and seal with nail polish. Let dry.
15. Image

